"Dimethylsulfide Oxidation over the Tropical South Atlantic: OH and other Oxidants"

Final Report
NASA-Stanford Joint Research Initiative Program

NASA Cooperative Agreement No. NCC2-5023

Brooke L. Hemming
Department of Chemistry
Stanford University

John A. Vastano
and
Robert B. Chatfield
NASA-Ames Research Center

Meinrat O. Andreae
Max Planck Institute for Chemistry

Lynn M. Hildemann
Department of Civil Engineering
Stanford University

Department of CIVIL ENGINEERING
STANFORD UNIVERSITY

INTRODUCTION: DMS and Cloud Formation in the Remote Marine Boundary Layer

The general course of events in the formation of a marine cloud begins with the emission of species which can eventually serve as nuclei around which water can condense to form a cloud droplet. In remote marine regions, cloud condensation nuclei (CCN) are primarily composed of sulfate, in either its acid or ammonium salt form. Most sulfate in these regions is the product of atmospheric oxidation of dimethyl sulfide (DMS), a reduced sulfur gas that is released by phytoplankton at the ocean surface. Therefore, in order to effectively quantify the links in the cloud-formation cycle, one must begin with a well-defined description of the atmospheric chemistry of DMS. The intent of this project has been to initiate development of a comprehensive model of the chemistry and dynamics responsible for the formation of clouds in the remote marine boundary layer. The primary tool in this work has been the Global/Regional Atmospheric Chemistry Event Simulator (GRACES), a global atmospheric chemistry model, which is under development within the Atmospheric Chemistry and Dynamics Branch of NASA-Ames Research Center. In this effort, GRACES was used to explore the first chemical link between DMS and sulfate by modeling the diurnal variation of DMS.

BACKGROUND: Previous Efforts to Model the DMS Diurnal Oxidation Cycle

Examples of other efforts to model the diurnal variation of DMS are described in M.O. Andreae, et al. [1985], Koga and Tanaka [1993], Saltzman, et al. [1993], Yvon, et al. [submitted, 1994], and Suhre and Rosset [1994]. Recent efforts to model the rate of formation of CCN [Russell, et al. 1994; Suhre and Rosset, 1994], treat the initial oxidation of DMS as manifested by its diurnal cycle in a limited fashion, assuming a parameterization that does not account for variations in flux and background atmospheric chemical composition. In this work, we consider these factors and the role they may play in dictating the rate of DMS oxidation.

The following questions have been considered in this study: 1) How well can a zero-dimensional chemical model predict the air concentrations of dimethylsulfide (DMSa) that were measured by the Andreae group [1994]? What are the implications, by extension, for higher dimensional DMS-CCN models which use zero-dimensional or simpler calculations as a first step in calculation? 2) Are there other significant sinks for DMS besides hydroxyl radical (OH)? 3) Is there evidence of a photoactive oxidant which becomes active at sunrise?

APPROACH:

The Data

The data considered in this study is composed of a 6-week continuous set of measurements including hourly atmospheric and sea water concentrations of DMS, ozone, air temperature, solar radiation, as well as half-daily radiosonde measurements of the marine boundary layer height [Andreae, et al., 1994]. DMS flux values were calculated using the measured wind speed, sea water temperature and the sea water DMS concentration. This data set was collected during a period of remarkably stable meteorological conditions, resulting in clear diurnal variation in hourly atmospheric DMS (DMSa) measurements. Analysis of the daily averages of the DMSa measurements versus the calculated DMS flux for February 12 through March 13 shows a strong correlation ($r^2 = 0.91$). An average of the hourly atmospheric DMS measurements taken during the March 8 - 16 period have been used in a one-dimensional modeling study of sulfur chemistry and aerosol formation in the marine boundary layer [Suhre, et al., 1994].

The GRACES -DMS Diurnal Variation (GRACES-DDV) Model

The primary oxidant of DMS is expected to be hydroxyl radical (OH). Nitrate radical (NO_3) is also thought to play a role in DMS removal at night. The concentrations of these and all other species are calculated by the GRACES model by integration of a full set of atmospheric reactions of importance in the troposphere. OH concentration is dependent upon the availability of ultraviolet light of the correct frequency to photolyze ozone. The photolysis rate of ozone and other photolyzible species is calculated using a δ-Eddington technique, modified for the presence of clouds, for an assigned surface albedo and for the solar radiation appropriate for the time of year and global location being modeled. These photochemical reaction rates are calculated based on tabulated absorption and quantum yield data. In this study, the ocean surface albedo was set to 0.1. The rates for non-photochemical reactions are derived from DeMore, et al., JPL evaluation, Atkinson, et al. IUPAC evaluation, the Paulson and Seinfeld condensed isoprene mechanism, Lurmann et al. condensed mechanism for C_2C_3, C_6-C_8(aromatic) species. Modifications to the hydrocarbon mechanism to include hydroperoxide chemistry were made as described in Chatfield and Delany. Rates for oxidation of DMS by OH and NO_3 radicals are those reported by Hynes, et al. [1986] and Atkinson, et al. [1992]. The full set of reactions is integrated by a differential-algebraic solver (DASSL) in fifteen minute time steps.

Chemical species are supplied to the model in two ways. All species are initially assigned a specific mixing ratio. Table 1. provides a list of the species and concentrations, as well as the temperature, standard altitude, gas number density and surface albedo used in a typical model calculation.

Table 1.

General Variables	
Altitude	3.3E+3 cm
Temperature	298.1 K
Number Density	2.4E+19 (#/cm^3)
Surface Albedo	0.1
Chemical Species	**Mixing Ratio**
H_20	2.39E-02
O_3	1.82E-8
NO	0
NO_2	5.00E-11
NO_3	0
HNO_2	0
CO	5.00E-8
CH_4	1.70E-6
H_2O_2	7.00E-10
HCl	1.00E-10
H_2	5.02E-7
DMS	1.23E-10
C_3H_6	3.60E-11
C_2H_4	5.60E-11
C_2H_6	5.60E-10
C_3H_8	3.60E-10
C_4H_8	5.00E-11

The values for CH_4, H_2, and H_2O_2 used are global averages. The mixing ratio for water was calculated from the daily dew points measured aboard the Meteor. Ozone (O_3) is maintained at its initial concentration by the model code to simulate its replenishment due to probable marine boundary dynamics. This assumption is made to fit observed concentrations. The ozone mixing ratio used was the average of the hourly measurements for the day being modeled. NOx and CO concentrations were estimated for the clean conditions observed during the cruise. Source terms for DMS and other reactive non-methane hydrocarbons are modeled as "appearance" rates, calculated from measured fluxes in the case of DMS or from measured background values for ethane (C_2H_6), ethene (C_2H_4), propane (C_3H_8), propene (C_3H_6) and butene (C_4H_8). Here it is assumed that the background concentrations of other biogenic hydrocarbons are proportional to the DMS background value. Rudolph and Johnen, in 1990, measured light hydrocarbons in the

central Atlantic region crossed at the mid-point of the Meteor cruise. Andreae, et al. measured DMSa concentrations that were a factor of two smaller than those measured in the part of the cruise of primary interest in this study. Hence, a simple estimate was made that the background levels of the light non-methane hydrocarbons in the region considered here are double those measured by Rudolph and Johnen. Appearance rates were then calculated to maintain a steady state against removal by OH at its daily average concentration. Table 2. lists the non-methane hydrocarbon source terms included in the model and the base values from which they were estimated.

Table 2.

Chemical Species	Low Productivity, Measured (ppt)	Mod. Productivity, Estimated (ppt)	Mod. Source Rate, Calc. (#/cm3*s)
Ethene (C_2H_4)	25[1]	50	6.5E+4
Ethane (C_2H_6)	278[1]	556	2.5E+6
Propene (C_3H_6)	18[1]	36	1.6E+5
Propane (C_3H_8)		360	5.9E+6
Butene (C_4H_8)	25[2]	50	

1. Rudolph and Johnen, JGR 95(D12), p. 20583, November 20, 1990.
2. Donahue and Prinn, 1990.

To calculate a DMS appearance rate from the hourly flux measurements taken aboard the Meteor, the average of the radiosonde measurements which gave a marine boundary layer height of 700 m was used. Here, the assumption was made that the marine boundary level is instantaneously well-mixed.

Since the principal focus of this work is the chemistry of DMS oxidation, the model is operated in its 0-dimensional mode. It is assumed that the diurnal change in DMS concentration can be calculated from the difference between the source term and its loss by chemistry. In this study, DMS dry and wet depositional processes are considered unimportant, due to its extremely low solubility in sea and cloud water. Other loss processes such as vertical entrainment by clouds at the top of the marine boundary layer will be considered later. Depositional losses of other species are also not considered within the model at present.

Analysis of the Meteor Dataset

As indicated above, the primary assumption in GRACES-DDV 0-dimensional chemical model is that the sole source of DMS is due to its flux from the ocean surface and its removal is due exclusively to oxidation. Thus, a correlation necessarily exists in the model between the rate

of flux and the concentration of DMS. In order to determine the impact of chemistry on the atmospheric DMS concentration, a data set which shows a strong correlation between flux and DMSa is required. Given the strong correlation between average daily DMS concentration and average daily DMS flux rate shown by Andreae, et al., an effort was made to determine the degree to which the hourly flux values correlated with the hourly DMSa measurements for individual days within their data set. The measured flux and DMSa values were plotted and a linear regression calculated for each day. The individual days which gave the best linear correlations, i.e. $R > 0.8$, were modeled, along with the subset chosen for modeling by Suhre, et al [1994].

Individual days were also normalized against their average DMS concentration, as a means of comparing the relative change in DMSa observed in the data, versus the change calculated in the model.

Furthermore, because the chemistry of interest in this study is thought to occur at specific times within the solar day, a similar analysis of the flux versus DMSa for night, early morning, mid- and late day was carried out. Individual days were divided into these time regimes according to flux of ultraviolet radiation measured on the particular day. Night time was defined as the periods beginning at midnight until sunrise and one hour after sunset through the following midnight. Early morning was chosen as the first 2-3 hours starting at sunrise and ending at the midpoint of the rising edge of the UV flux curve. Midday was contained between the midpoints of the UV flux rise and fall. Late day was the interval between the end of the midday period and sunset. Table 3. shows the hours selected for each interval by date.

Table 3.

Date	Night-time	Early Morning	Midday	Late Day
February 20	0-7, 21-23	8-10	11-17	18-20
February 28	0-5, 19-23	5-8	9-15	16-18
March 4	0-6, 19-23	7-9	10-15	16-18
March 8	0-5, 18-23	6-7	8-15	16-17
March 9	0-5, 18-23	6-7	8-15	16-17
March 10	0-5, 19-23	6-7	8-16	17-18
March 11	0-4, 18-23	5-6	7-15	16-17
March 12	0-5, 19-23	6-7	8-16	17-18
March 13	0-5, 19-23	6-7	8-16	17-18
March 14	0-5, 19-23	6-7	8-16	17-18
March 15	0-4, 18-23	5-6	7-15	16-17
March 16	0-4, 18-23	5-6	7-15	16-17

The linear rate of change in DMS concentration at early morning and midday was also calculated explicitly for both the model and data for individual days.

Model Calculations Undertaken

A subset of daily measurements was modeled, using the 24 hour average flux, ozone, DMS level, water mixing ratio and air temperature for each day. The model was also provided with the latitude, longitude and date which the measurements were taken to assure that appropriate solar radiation flux values were used in the photochemical rate calculations. Flux to DMSa correlation plots were constructed and the change in early/midday DMS was calculated for comparison to the data. Table 4. shows the measured variables used in the model calculations.

Table 4.

Date	DMS Flux[1]	DMSa[2]	Ozone[3]	Water[4]	Air Temp[5]	Latitude[6]	Long.[6]
Feb 20	2.81	32.35	14.12	2.30	25.75	-18.63	-24.94
Feb 28	3.50	56.42	13.35	2.40	25.00	-22.82	-14.91
Mar 4	9.15	155.6	9.458	2.38	24.32	-19.60	-6.761
Mar 8	8.90	138.5	16.33	2.32	24.12	-19.00	-0.332
Mar 9	8.32	133.9	18.61	2.39	24.95	-19.00	1.34
Mar 10	9.30	146.9	18.17	2.27	23.22	-19.00	3.00
Mar 11	13.9	193.8	17.05	2.26	23.05	-19.00	4.72
Mar 12	19.7	167.3	17.73	2.18	22.62		
Mar 13	24.3	129.2	18.47	1.93	22.03		
Mar 14	14.2	99.22	18.58	1.77	21.82		
Mar 15	13.6	111.9	19.17	1.88	21.95		
Mar 16	13.8	139.2	21.37	1.82	21.63		

Units

1. $\mu mol/m^2*day$ --- mean measured value for given day
2. parts per trillion --- mean measured value for given day
3. parts per billion --- mean measured value for given day
4. percentage by number --- mean measured value for given day
5. Celsius --- mean measured value for the given day.
6. degrees --- location of the ship at noon on the given day

General calculations were performed to assess the relative importance of each of the key variables in determining the calculated concentration of DMS. The sensitivity of OH concentration to CO concentrations between 40 and 60 ppb and NOx concentrations between 5 and 50 ppt was evaluated. For a direct assessment of the consequences to the DMS concentration, the model was supplied with a +/- 20% range around the measured or estimated

values of DMS flux, ozone, water, carbon monoxide and nitrogen oxides. This calculation was especially useful in estimating the impact due to error in the guessed values of NOx and carbon monoxide, which were not measured aboard the Meteor.

Given the interest shown in the atmospheric chemistry literature in the possibility of a halogen-based, photochemically active oxidant, an evaluation of the behavior of such an oxidant on the diurnal variation of DMS was carried out. A source term and the necessary photolysis rate information for hypochlorous acid (HOCl), a gas-phase species that might evolve from acidified sea salt aerosol, was included in the model. Due to the photochemical similarity expected between HOCl and HOBr, this evaluation is also relevant to HOBr.

RESULTS

Table 5. Correlation statistics for hourly DMSa vs. DMS flux values measured by day.

Date	Julian Date	Slope	R Value
February 12	31819	-2.77	0.436
February 13	31820	-7.22	0.393
February 14	31821	6.26	0.630
February 15	31822	13.7	0.533
February 16	31823	10.3	0.620
February 17	31824	4.23	0.440
February 18	31825	0.602	0.0232
February 19	31826	2.63	0.337
February 20 *	31827	15.1	0.895
February 21	31828	3.49	0.129
February 22	31829	22.9	0.740
February 23	31830	15.6	0.721
February 24	31831	0.665	0.0574
February 25	31832	-2.13	0.126
February 26	31833	6.39	0.330
February 27	31834	11.6	0.384
February 28 *	31835	22.0	0.816
March 1	31836	-1.67	0.0345
March 2	31837	11.6	0.688
March 3	31838	8.50	0.477
March 4 *	31839	10.8	0.831
March 5	31840	-2.80	0.281
March 6	31841	17.41	0.794
March 7	31842	5.56	0.322
March 8 *	31843	8.56	0.392
March 9 *	31844	8.96	0.900
March 10 *	31845	-2.26	0.159
March 11 *	31846	2.45	0.336
March 12 *	31847	2.91	0.248
March 13 *	31848	0.378	0.129
March 14 *	31849	-0.852	0.149
March 15 *	31850	0.679	0.167
March 16 *	31851	-0.603	0.0707
March 17	31852		
March 18	31853		
March 19	31854		
March 20	31855		
March 21	31856		

In addition to the subset modeled by Suhre, et al. (March 8-16), February 20, February 28 and March 4 were also chosen for calculation as having shown the best linear correlation between flux and DMSa.

Figures 1-12 show the results of the model calculations in relation to the hourly DMSa measurements. For comparison, DMS and UV flux are also shown. Figure 13 is a plot of the difference in DMS concentration, normalized for average background DMS, between the data and the model for the four most highly correlated days. Figure 14 shows the linear correlation between flux and DMSa for the data and the model for the same set of days. Figure 15 compares the model with the March 8-16 data set. Table 6. summarizes the amplitude, length and mean DMS values for the diurnal cycles modeled

Table 6. Variablity in DMSa by day: Measured and Modeled

Date	Cycle Amp. Data	Cycle Amp. Model	Cycle Leng. Data	Cycle Leng. Model	Mean DMS Data	Mean DMS Model
Feb 20	1.1005	1.2200	13.300	6.8000	32.350	32.940
Feb 28	1.0886	1.2572	11.400	7.2500	56.420	51.350
March 4	0.77410	1.0500	12.770	7.4000	155.59	160.80
March 8	0.67500	1.4370	10.030	7.1300	138.50	127.80
March 9	0.61100	1.5257	9.0100	6.8300	133.94	110.36
March 10	0.81850	1.4938	9.9000	6.7300	146.90	127.44
March 11	0.80090	1.4357	11.350	7.1300	193.80	203.67
March 12	0.99800	1.3228	13.320	6.4300	167.26	218.97
March 13	0.56790	1.1792	10.310	6.5300	129.20	262.36
March 14	0.80500	1.2542	10.270	6.9000	99.220	184.41
March 15	0.58900	1.3287	8.8500	6.7000	111.89	175.93
March 16	0.72590	1.3874	9.5800	6.7300	139.21	172.34

Figure 16. compares the ratios of maximum measured to minimum measured DMSa to the same ratio calculated for the models of oxidation of DMS by OH alone, OH and NO3 with 50 ppt NOx and 100 ppt NOx present, respectively. The impact on the model trace by variation of certain key variables is shown in Figures 17-19. Figure 20 shows the values for OH calculated by GRACES for a range of initial carbon monoxide and nitrogen dioxide concentratons. Figure 21 shows the partitioning of NOx within a 24-hour period within the model. Table 7 gives a comparison between the rates of change with time in DMS at midday (10AM-2PM) when the OH concentration is expected to be highest. These rates were calculated as linear fits to the data and model in this time interval.

Table 7.

Date	Slope (Data)	R Value (Data)	Slope (Model)	R Value (Model)
Feb 20	-4.63	0.994	-5.44	0.967
Feb 28	-7.52	0.971	-11.7	0.981
March 4	-4.68	0.925	-32.5	0.991
March 8	-8.18	0.684	-31.9	0.973
March 9	-14.1	0.915	-27.5	0.963
March 10	-22.3	0.991	-32.1	0.967
March 11	-13.0	0.986	-52.1	0.975
March 12	-14.5	0.952	-53.2	0.975
March 13	-7.49	0.775	-61.1	0.981
March 14	-10.2	0.985	-43.8	0.981
March 15	-7.46	0.921	-43.0	0.976
March 16	-22.1	0.951	-42.9	0.972

Figures 22-25 show the results of the comparison of data to model for photochemically interesting time regimes. Parts a. are correlation plots for March 8-16. Parts b. are correlation plots for Feb 20, Feb 28, March 4 and March 9.

Figures 26 and 27 show the results of a modeling of HOCl/HOCl source terms that are 25%, 50% and 100% of the DMS source strength.

CONCLUSIONS, to date:

The model consistently overpredicts the morning, and underpredicts the late afternoon concentration of DMS in all cases considered. The afternoon underpredication may be remedied by inclusion of a more complete sulfur oxidation mechanism than currently exists in the model. The consequence will be a larger sink for OH as the DMS oxidation products react further. At this juncture, it appears that an early morning drop off in measured DMSa that is not predicted by this chemical model. Due to the difficulty in finding a large set of days with a strong DMSa to flux correlation, it might be wise to consider the possibility of meteorological effects. The alternative suggestion is that a photochemically active oxidant accumulates at night, and then becomes active at sunrise. HOCl/HOBr behave photochemically in this manner, however, the source terms required to make a discernible difference in the modeled trace of DMS are so large as to be highly unrealistic.

Additional analysis is required to evaluate the days best modeled to determine the conditions under which a zero-dimensional model can be used most effectively to provide a DMS source for CCN. The time scales of chemistry and dynamics in the marine boundary layer must be factored into this analysis. It may be possible to adapt the GRACES model to allow for hourly changes in DMS flux, which may impact the ability of the model to fit the early morning DMSa concentration, in particular.

REFERENCES

Tracey W. Andreae, Meinrat O. Andreae, and Gunther Schebeske, "Biogenic sulfur emissions and aerosols over the tropical South Atlantic, 1. Dimethylsulfide in seawater and the atmospheric boundary layer," Journal of Geophysical Research, 99(D11), 22, 819-22,829, November 20, 1994.

Hynes, et al. (1986), J. Phys. Chem. 90, 4148.

Atkinson et al. (1992), J. Phys. Chem. Ref. Data 21, 1125.

DeMore, et al., JPL 92-20, Chemical Kinetics and Photochemical Data for Use in Stratospheric Modeling, August 15, 1992.

M. O. Andreae, R. J. Ferek, F. Bermond, K. P. Byrd, R. T. Engstrom, S. Hardin, P. D. Houmere, F. LeMarrec, H. Raemdonck and R. B. Chatfield, "Dimethyl Sulfide in the Marine Atmosphere," Journal of Geophysical Research, 90(D7), 12,891-12,900, December 20, 1985.

Seizi Koga and Hiroshi Tanaka, "Numerical Study of the Oxidation Process of Dimethylsulfide in the Marine Atmosphere," Journal of Atmospheric Chemistry, 17, 201-228, 1993.

E. S. Saltzman, D. J. Cooper, S.A. Yvon, M. O. Andreae, T. W. Andreae, A. R. Bandy, T. S. Bates, D. D. Davis, R. J. Ferek, J. E. Johnson, M. C. Shipham, and D. C. Thornton, "Diurnal Variations in Atmospheric Sulfur Gases Over the Western Equatorial Atlantic Ocean," Journal of Geophysical Research, in press, 1993.

S. A. Yvon, E. S. Saltman, D. J. Cooper, T. S. Bates, A. M. Thompson, "Atmospheric Dimethylsulfide Cycling at a Tropical South Pacific Station (12S, 135W): A Comparison of Field Data and Model Results," Journal of Geophysical Research (submitted).

Karsten Suhre and Robert Rosset, "DMS Oxidation and Turbulent Transport in the Marine Boundary Layer: A Numerical Study," Journal of Atmospheric Chemistry, 18, 379-395, 1994.

Figure 1.

Febuary 20, 1991

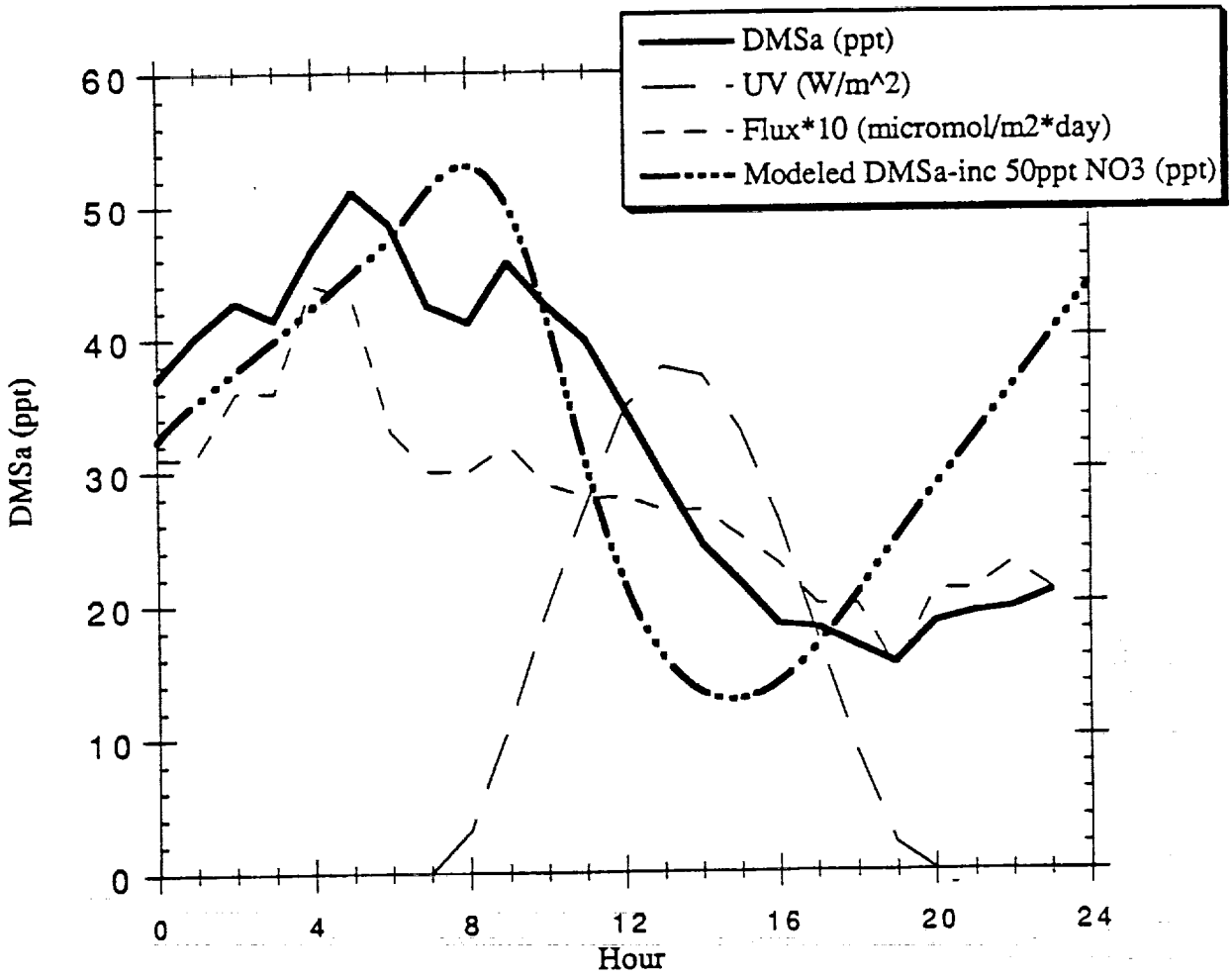

Figure 2.

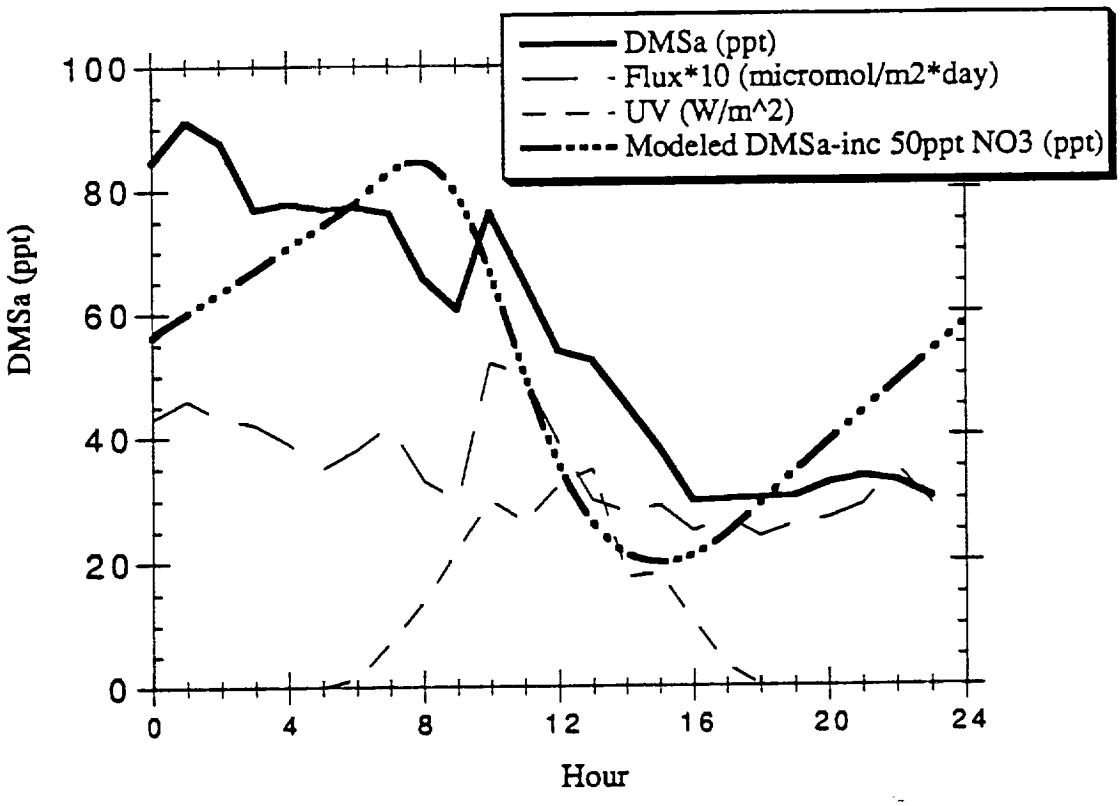
Feb 28, 1991
DMSa (ppt)
- Flux*10 (micromol/m2*day)
- UV (W/m^2)
Modeled DMSa-inc 50ppt NO3 (ppt)
DMSa (ppt)
100
80
60
40
20
0
0
4
8
12
16
20
24
Hour

Figure 3.

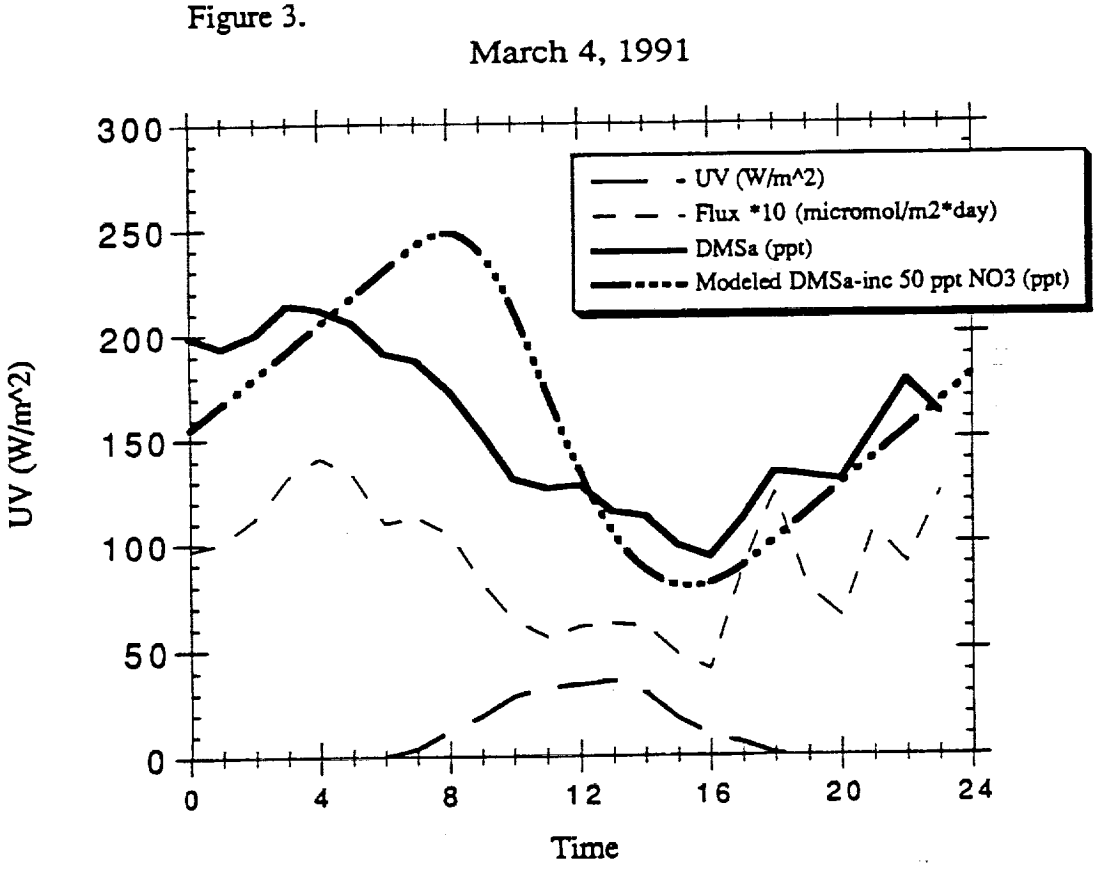
March 4, 1991
UV (W/m^2)
300
250
200
150
100
50
0
0
4
8
12
16
20
24
Time
- UV (W/m^2)
- Flux *10 (micromol/m2*day)
DMSa (ppt)
Modeled DMSa-inc 50 ppt NO3 (ppt)

Figure 4.

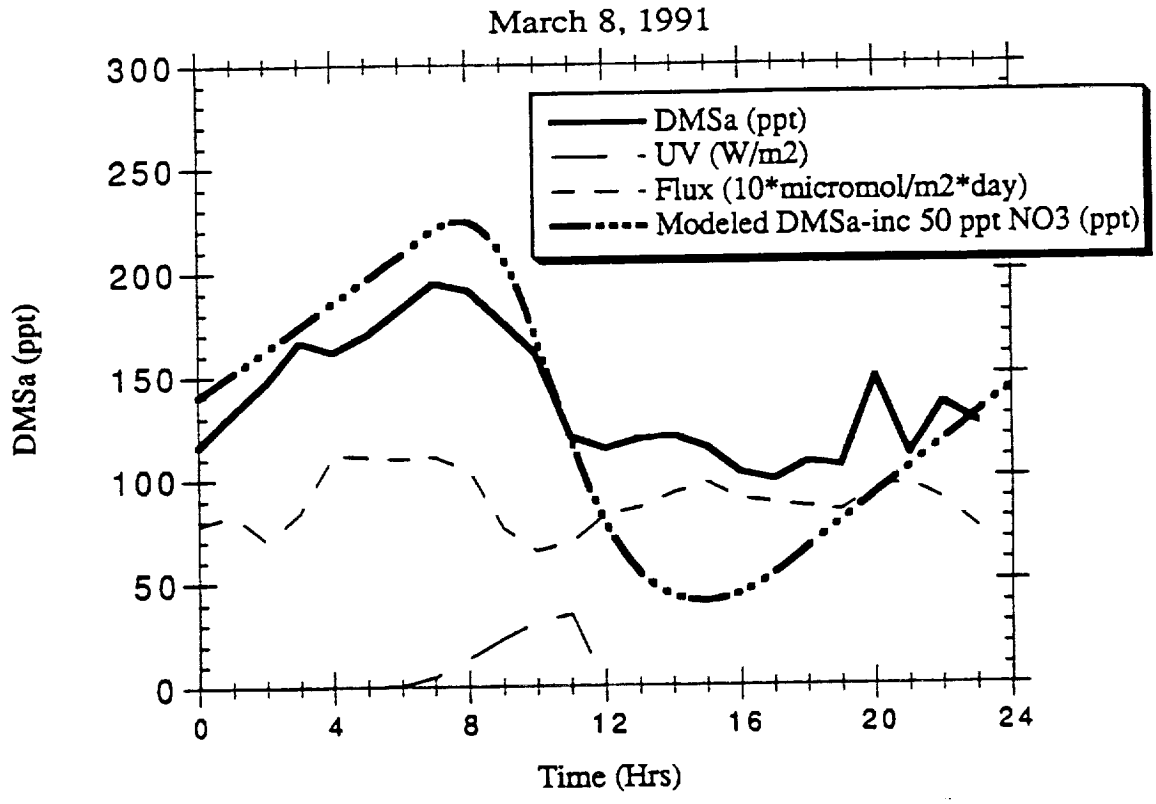
March 8, 1991
DMSa (ppt)
- UV (W/m2)
- Flux (10*micromol/m2*day)
Modeled DMSa-inc 50 ppt NO3 (ppt)
DMSa (ppt)
Time (Hrs)
300
250
200
150
100
50
0
0
4
8
12
16
20
24

Figure 5.

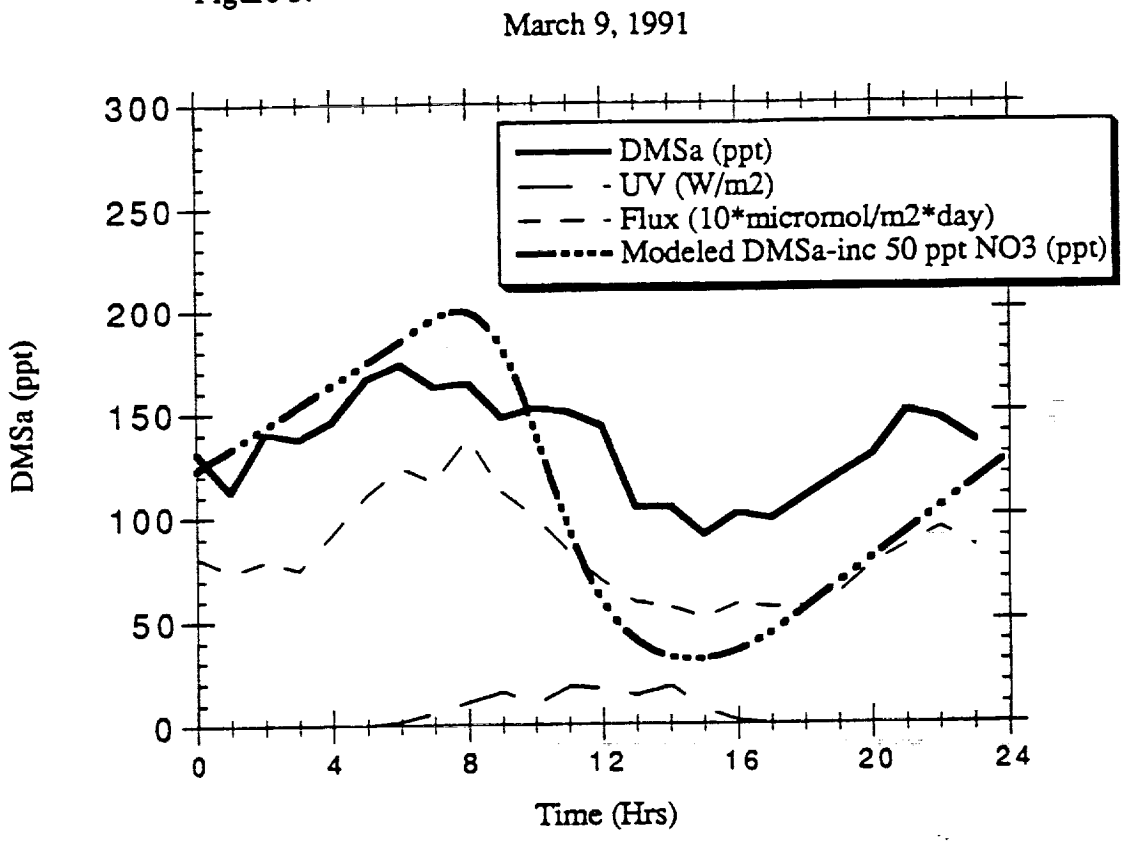
March 9, 1991
DMSa (ppt)
- UV (W/m2)
- Flux (10*micromol/m2*day)
Modeled DMSa-inc 50 ppt NO3 (ppt)
DMSa (ppt)
Time (Hrs)
300
250
200
150
100
50
0
0
4
8
12
16
20
24

Figure 6.

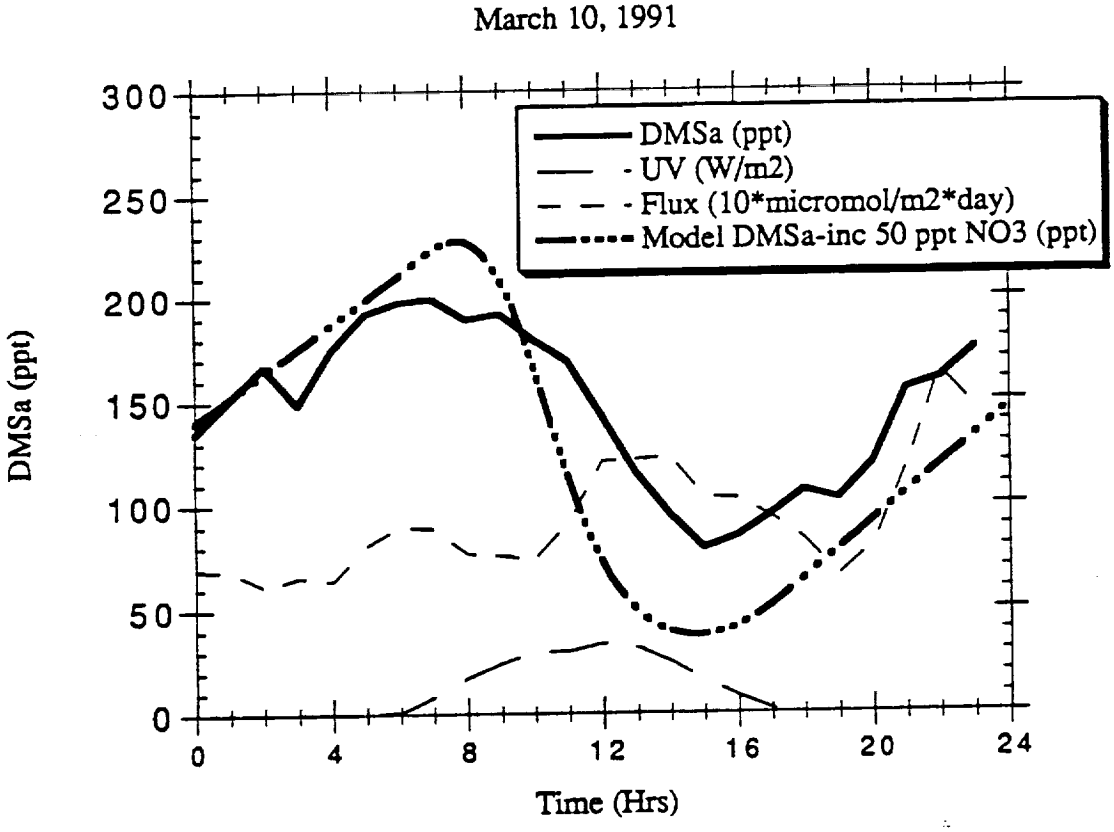
March 10, 1991
DMSa (ppt)
- UV (W/m2)
- Flux (10*micromol/m2*day)
Model DMSa-inc 50 ppt NO3 (ppt)
DMSa (ppt)
Time (Hrs)
300
250
200
150
100
50
0
0
4
8
12
16
20
24

Figure 7.

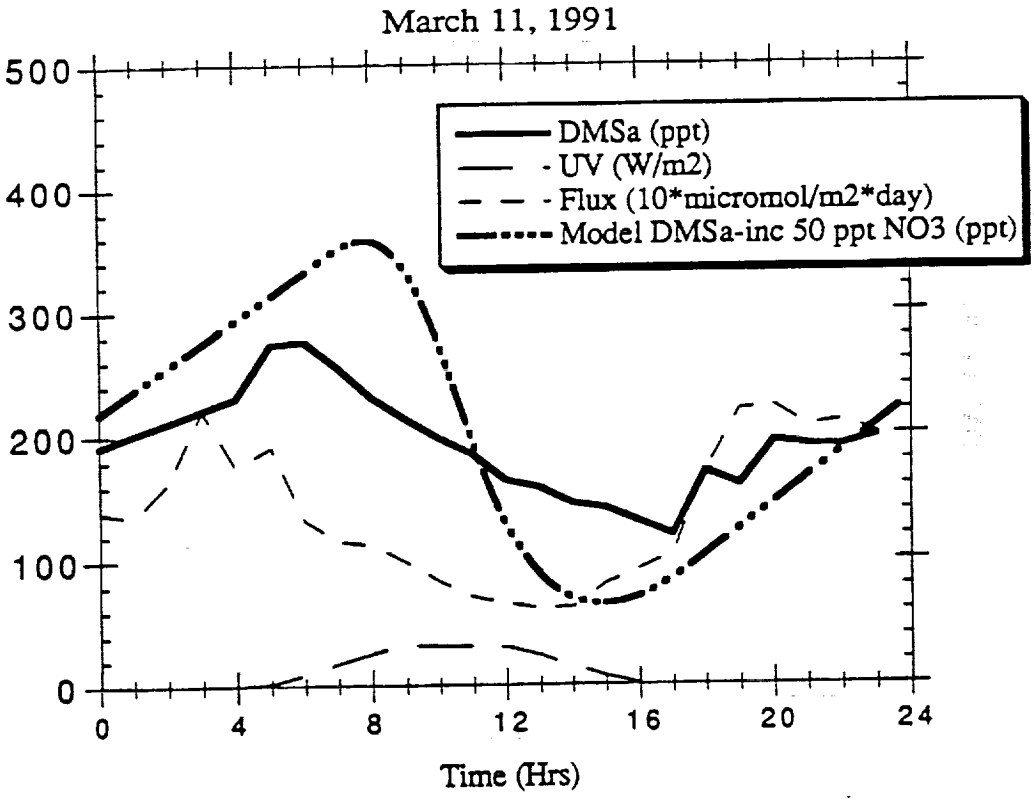
March 11, 1991
500
400
300
200
100
0
0
4
8
12
16
20
24
Time (Hrs)
DMSa (ppt)
- UV (W/m2)
- Flux (10*micromol/m2*day)
Model DMSa-inc 50 ppt NO3 (ppt)

Figure 8.

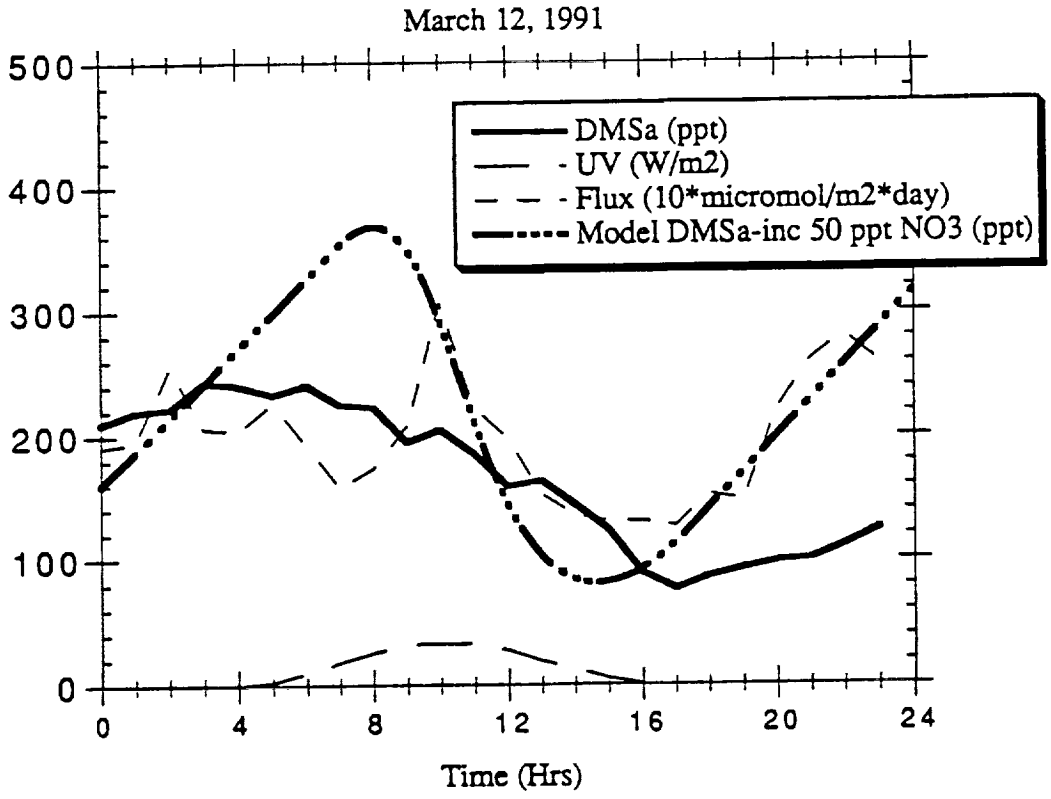
March 12, 1991
500
400
300
200
100
0
0
4
8
12
16
20
24
Time (Hrs)
DMSa (ppt)
- UV (W/m2)
- Flux (10*micromol/m2*day)
Model DMSa-inc 50 ppt NO3 (ppt)

Figure 9.

March 13, 1991

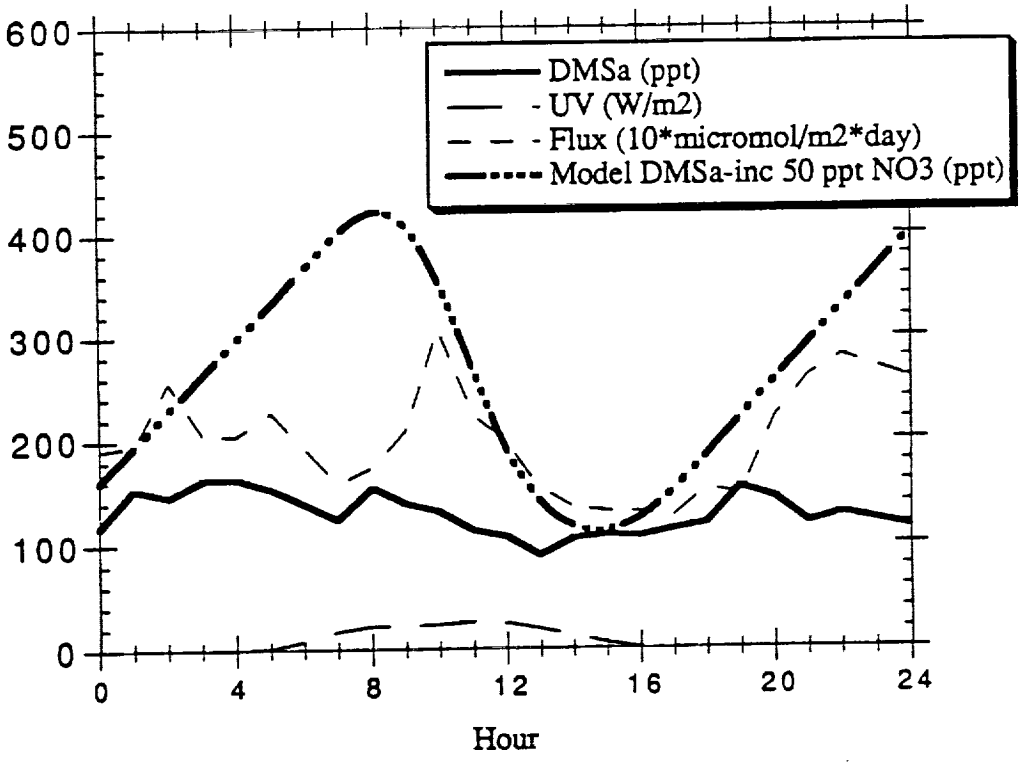

Figure 10.

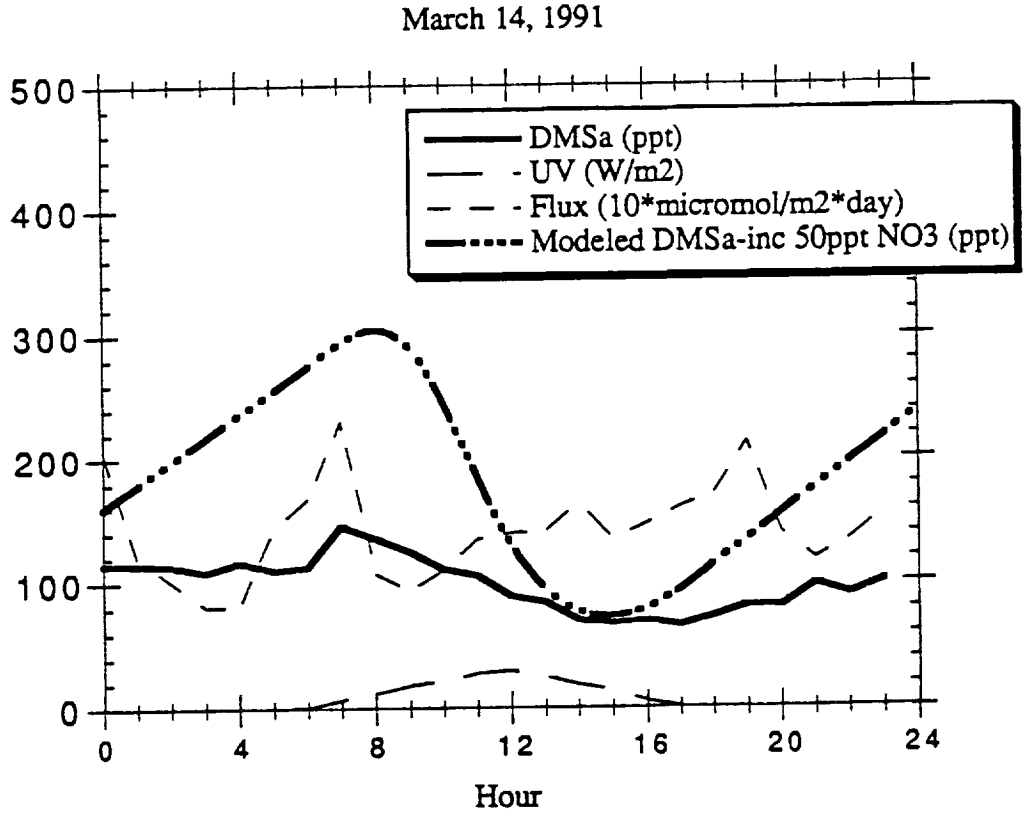
March 14, 1991
500
400
300
200
100
0
0
4
8
12
16
20
24
Hour
DMSa (ppt)
- UV (W/m2)
- Flux (10*micromol/m2*day)
Modeled DMSa-inc 50ppt NO3 (ppt)

Figure 11.

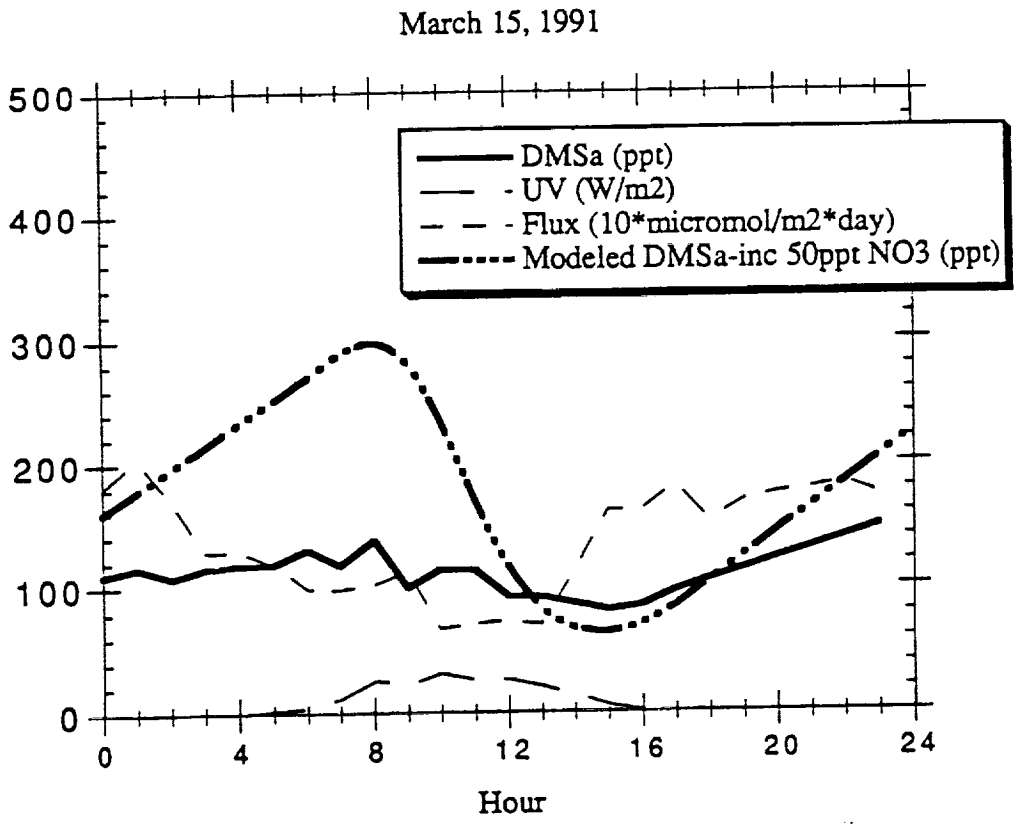
March 15, 1991
500
400
300
200
100
0
0
4
8
12
16
20
24
Hour
DMSa (ppt)
- UV (W/m2)
- Flux (10*micromol/m2*day)
Modeled DMSa-inc 50ppt NO3 (ppt)

Figure 12.

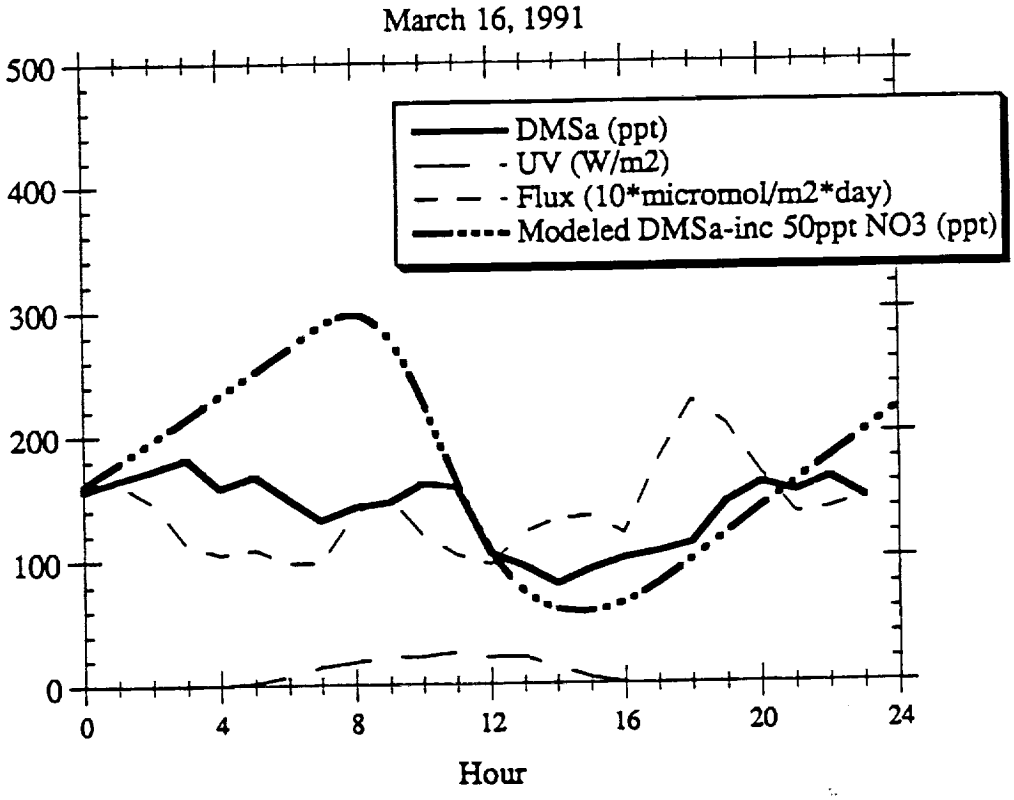
March 16, 1991
500
400
300
200
100
0
0
4
8
12
16
20
24
Hour
DMSa (ppt)
- UV (W/m2)
- Flux (10*micromol/m2*day)
Modeled DMSa-inc 50ppt NO3 (ppt)

Figure 13.

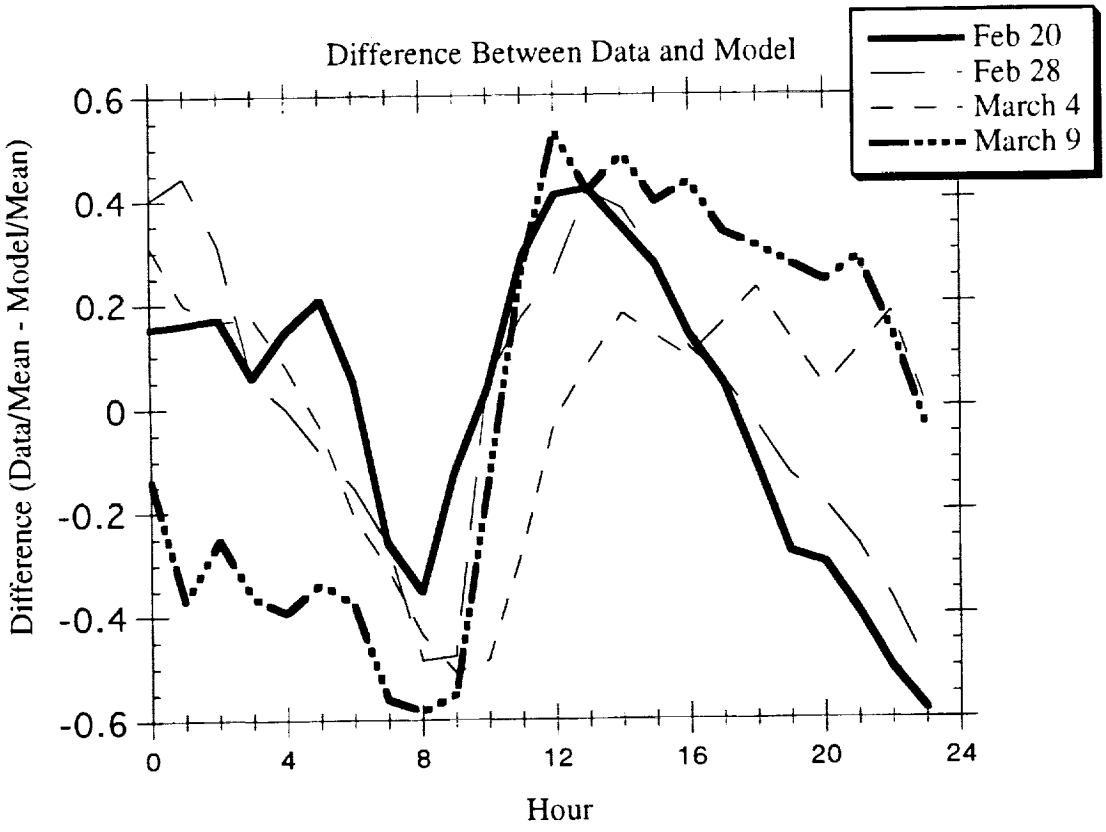
Difference Between Data and Model
Feb 20
Feb 28
March 4
March 9
Difference (Data/Mean - Model/Mean)
0.6
0.4
0.2
0
-0.2
-0.4
-0.6
0
4
8
12
16
20
24
Hour

Figure 14.

DMS Flux vs. [DMSa] : Data and Model

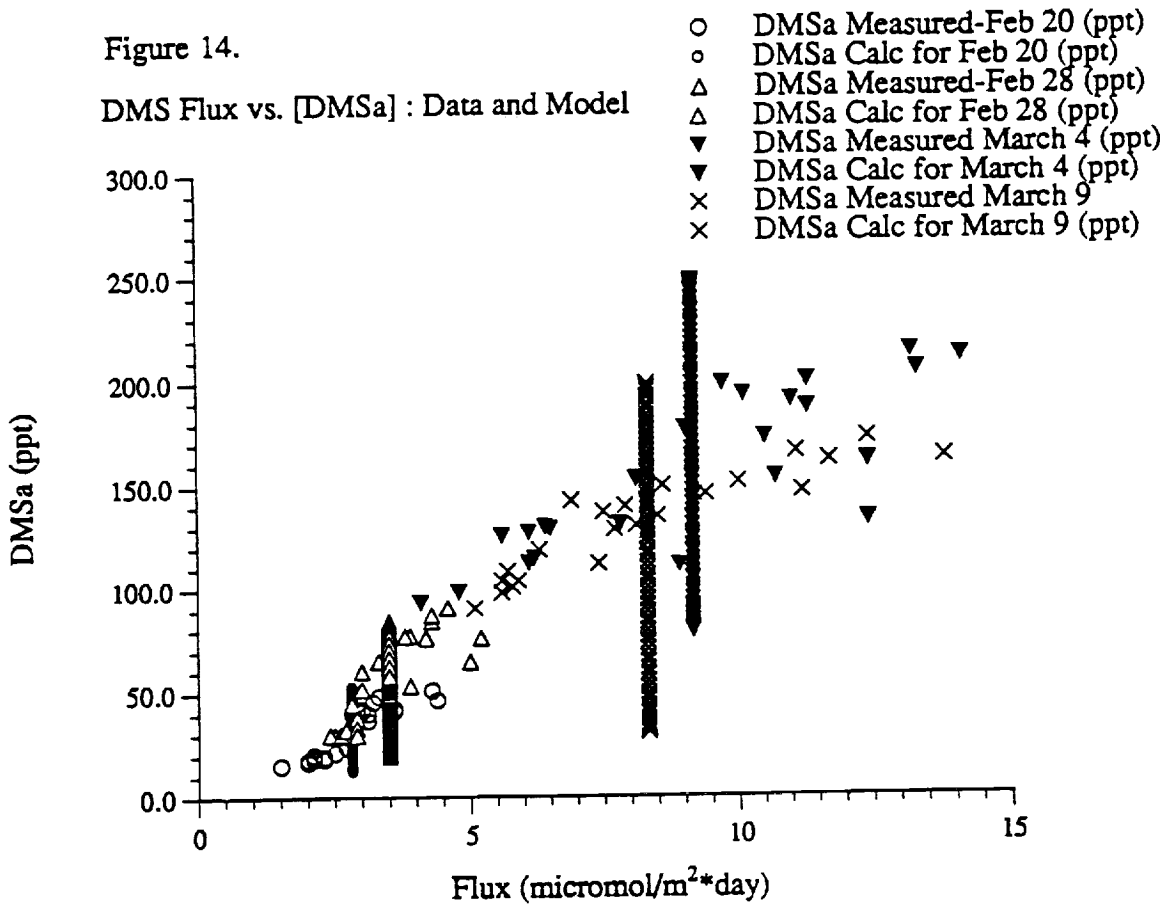

Figure 15a.

Flux vs. DMSa: Measured and Modeled

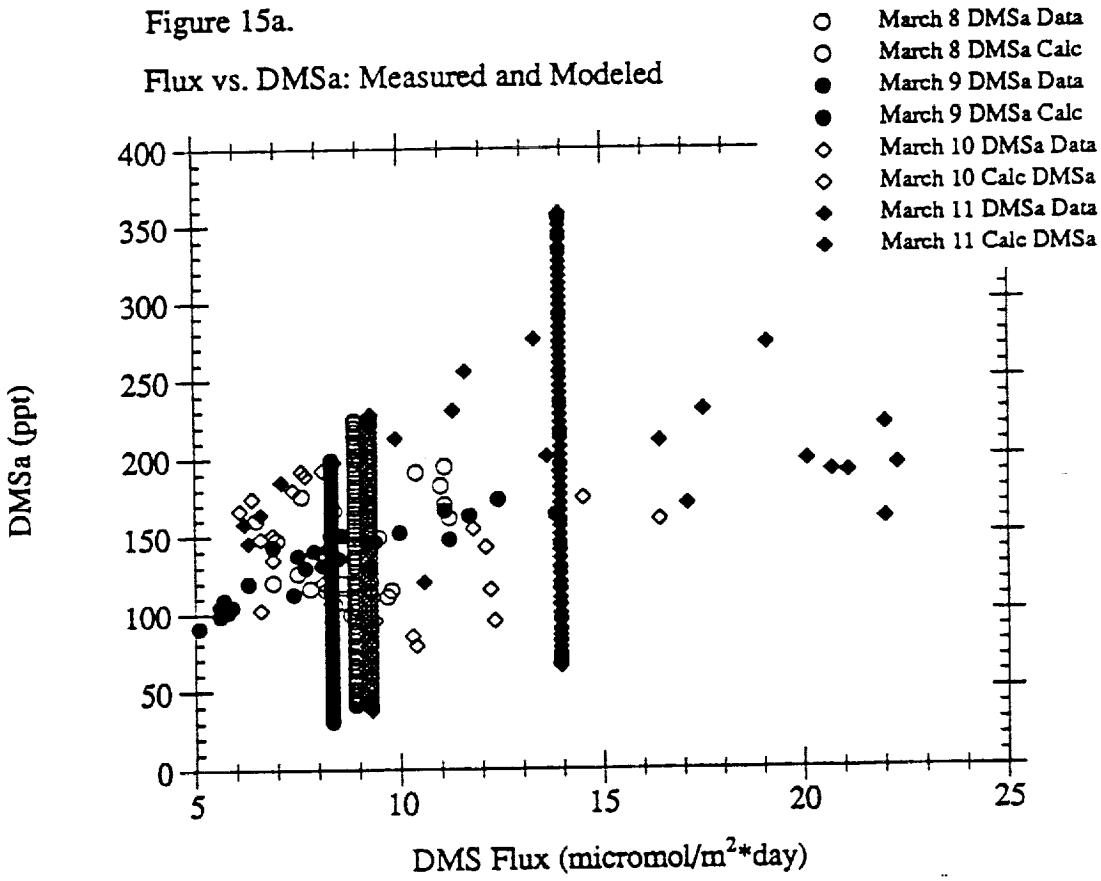

Figure 15b.

Flux vs. DMSa: Data and Model

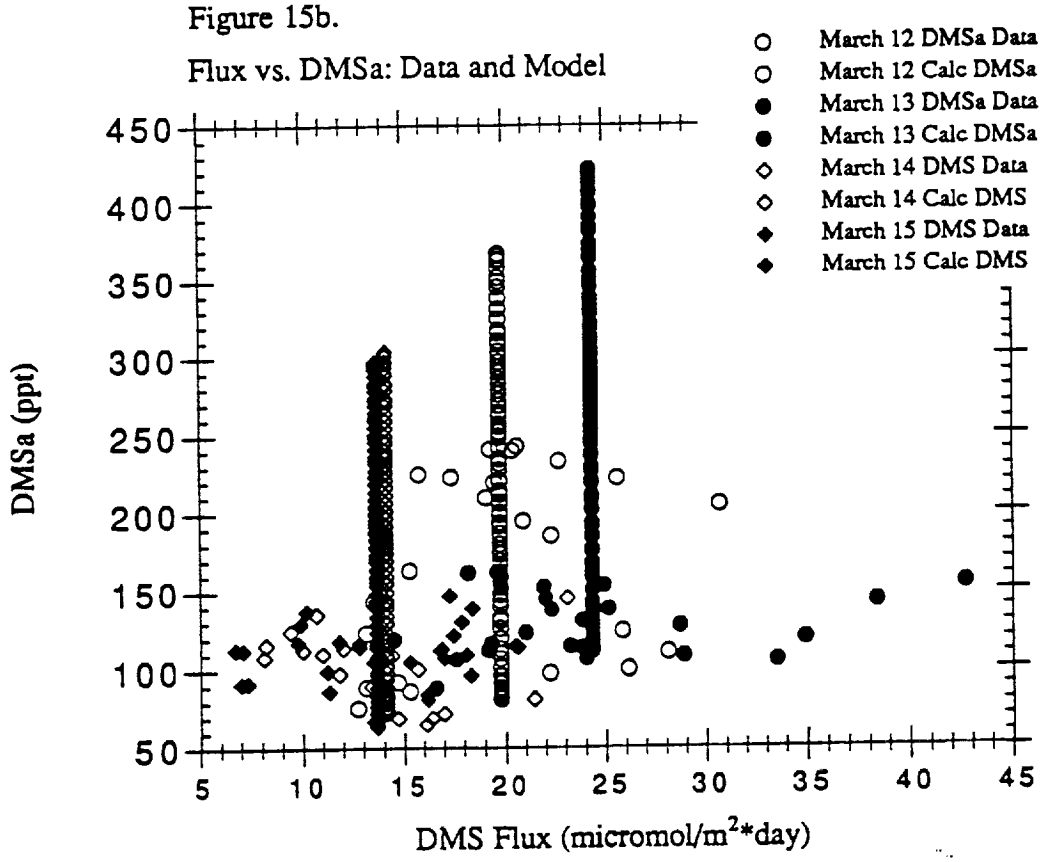

Figure 15c.

Flux vs. DMSa: Data and Model

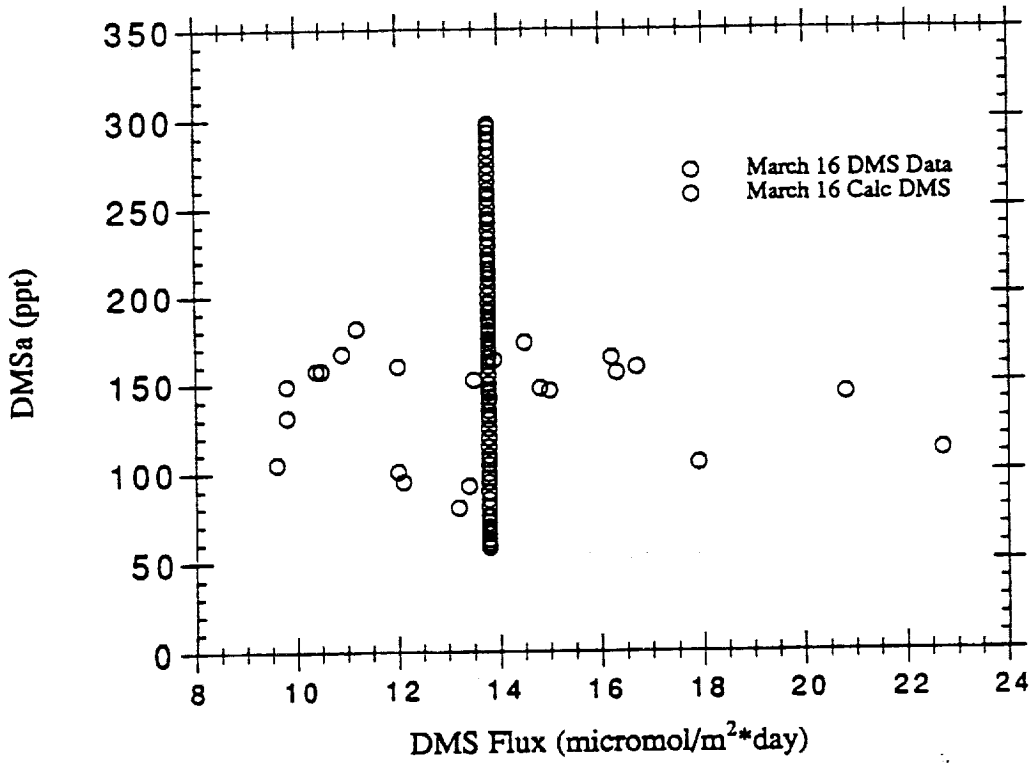

Figure 16.

Ratio of Maximum [DMSa] to Minimum [DMSa]): Data and Model

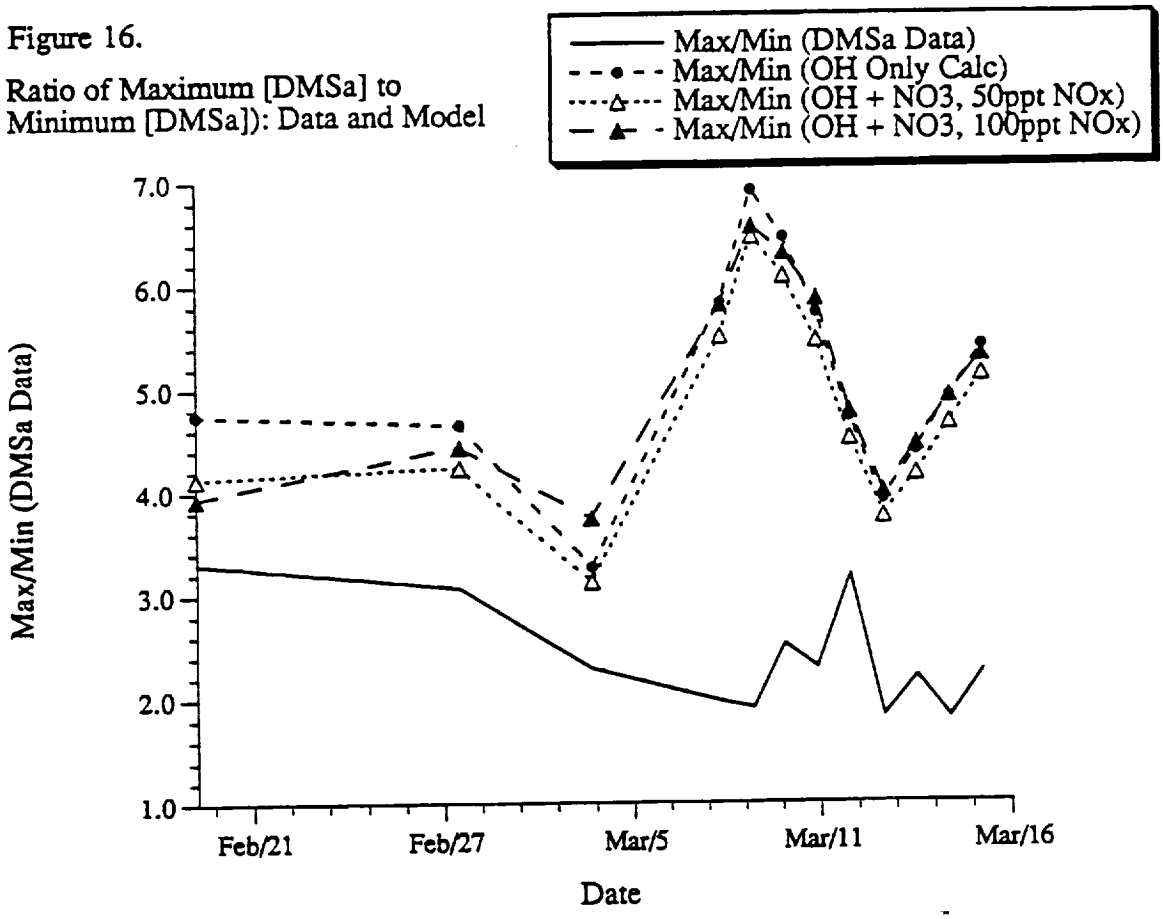

Figure 17.

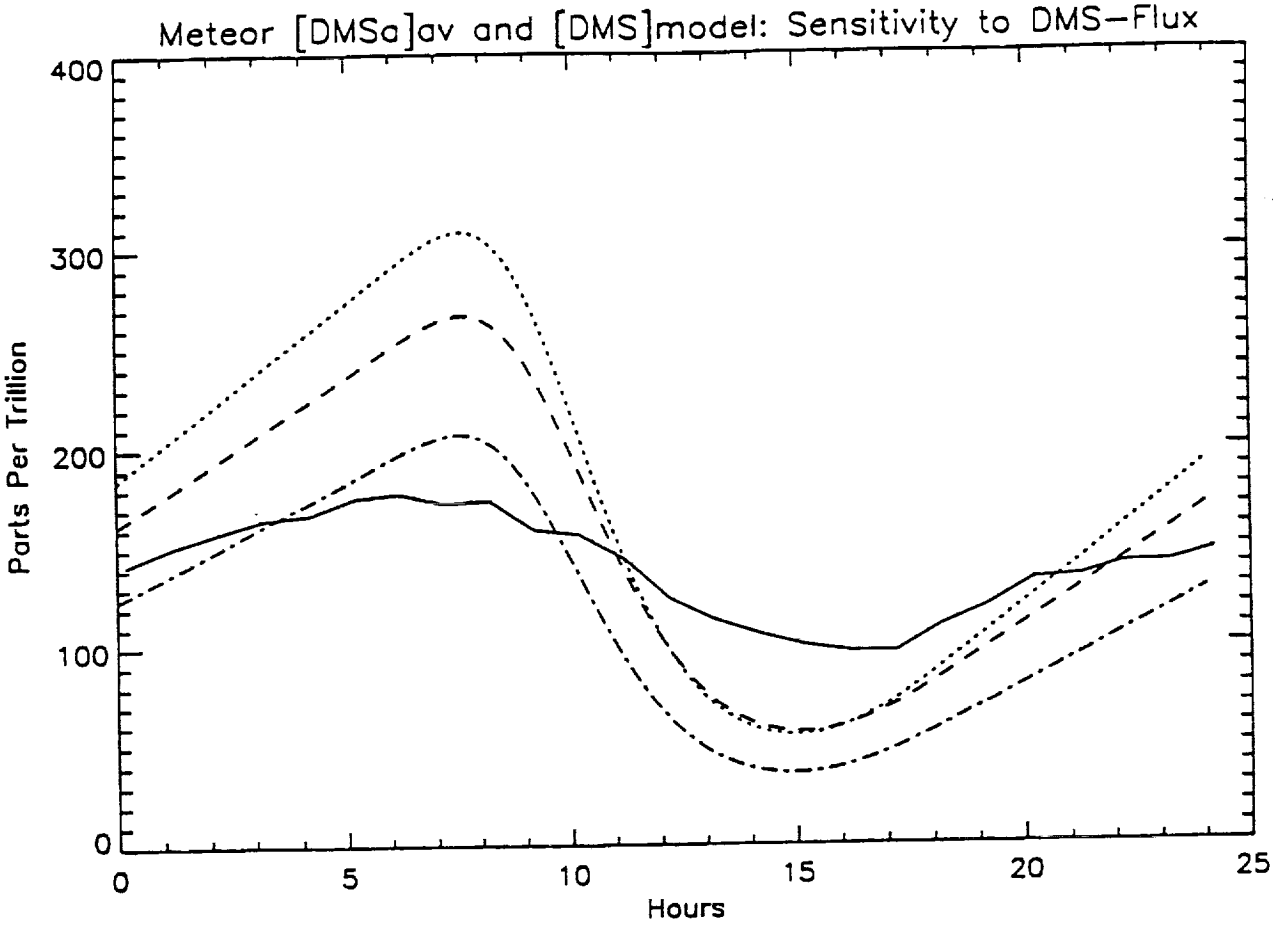
Meteor [DMSo]av and [DMS]model: Sensitivity to DMS−Flux
Parts Per Trillion
400
300
200
100
0
0
5
10
15
20
25
Hours

Figure 18.

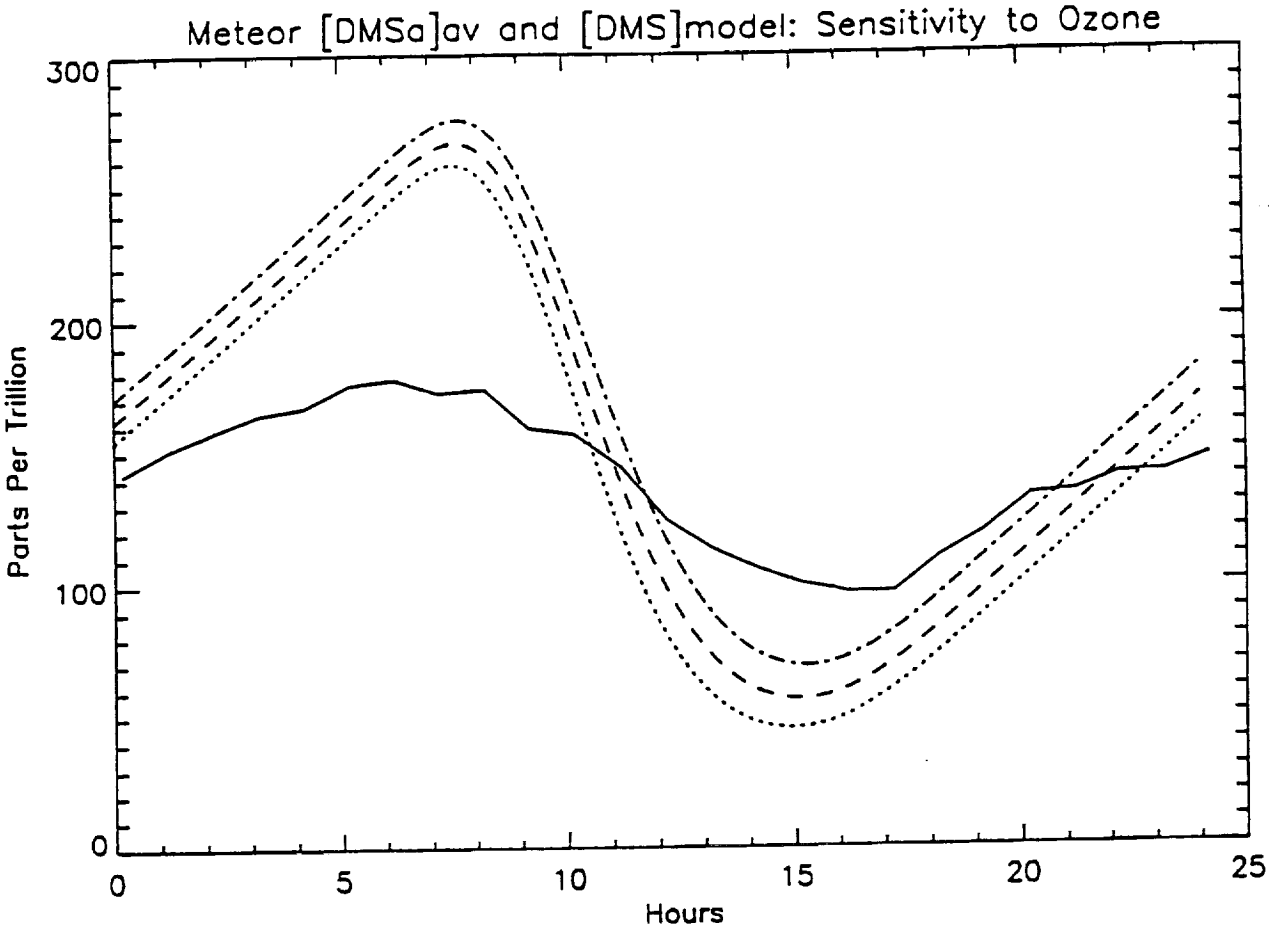
Meteor [DMSa]av and [DMS]model: Sensitivity to Ozone
Parts Per Trillion
300
200
100
0
0
5
10
15
20
25
Hours

Figure 19.

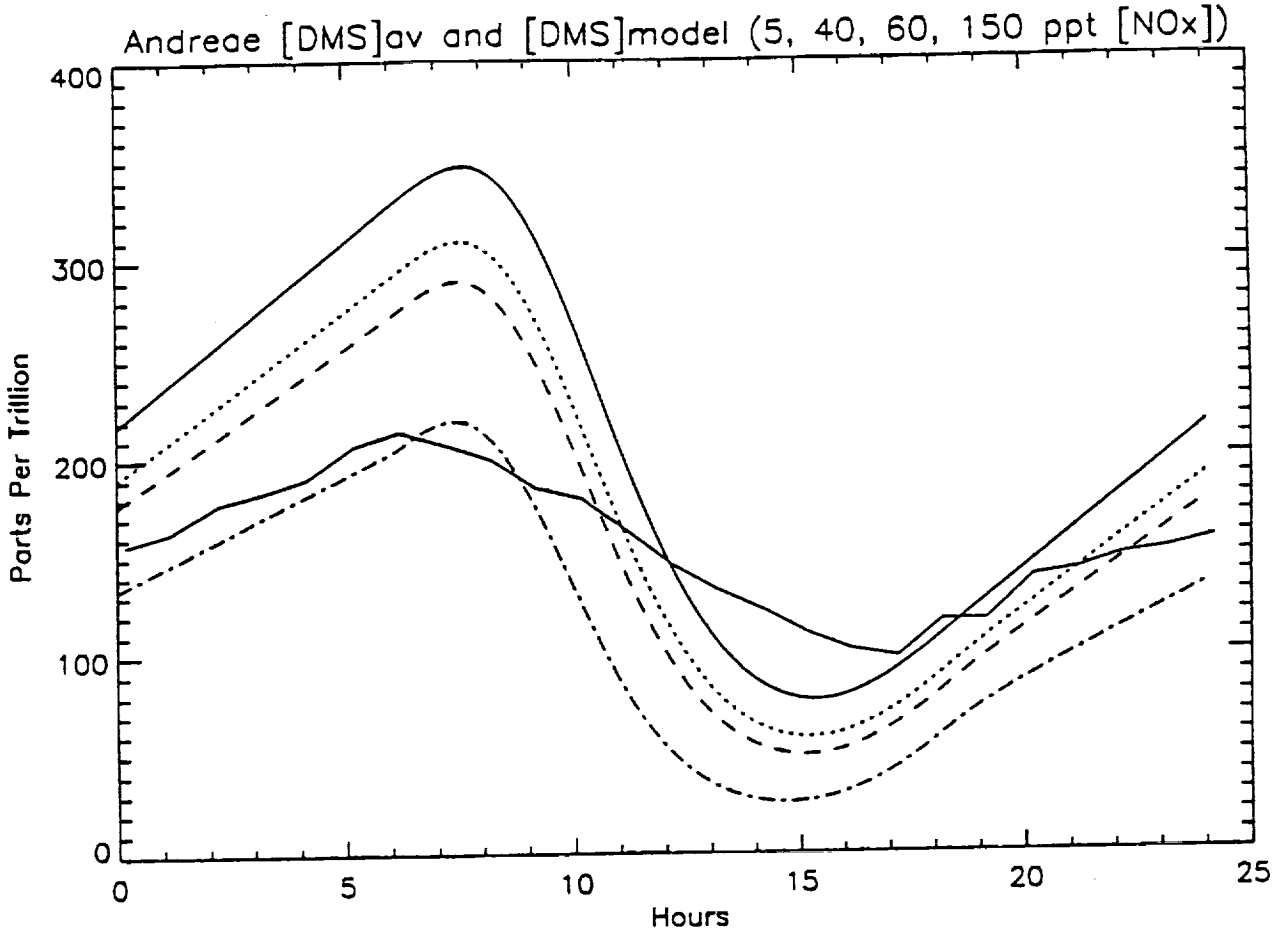
Andreae [DMS]av and [DMS]model (5, 40, 60, 150 ppt [NOx])
Parts Per Trillion
400
300
200
100
0
0
5
10
15
20
25
Hours

Figure 20.

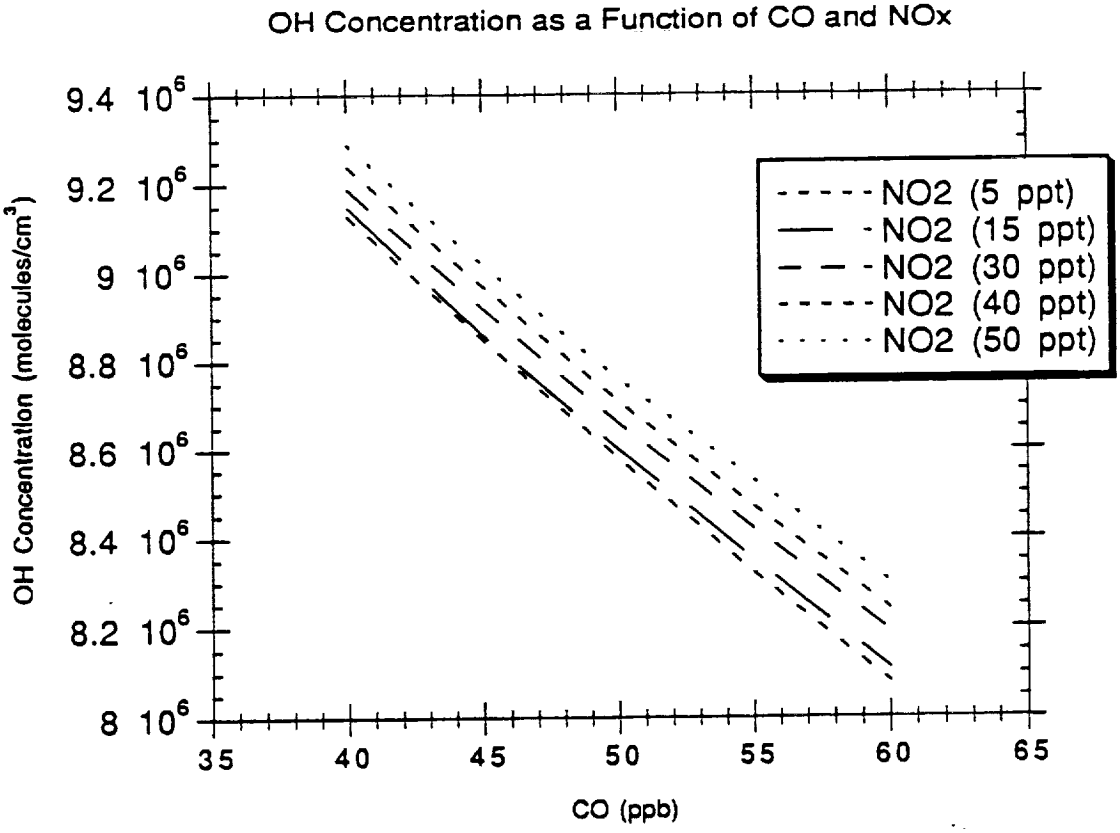
OH Concentration as a Function of CO and NOx
OH Concentration (molecules/cm^3)
9.4 10^6
9.2 10^6
9 10^6
8.8 10^6
8.6 10^6
8.4 10^6
8.2 10^6
8 10^6
35
40
45
50
55
60
65
CO (ppb)
NO2 (5 ppt)
NO2 (15 ppt)
NO2 (30 ppt)
NO2 (40 ppt)
NO2 (50 ppt)

Figure 21.

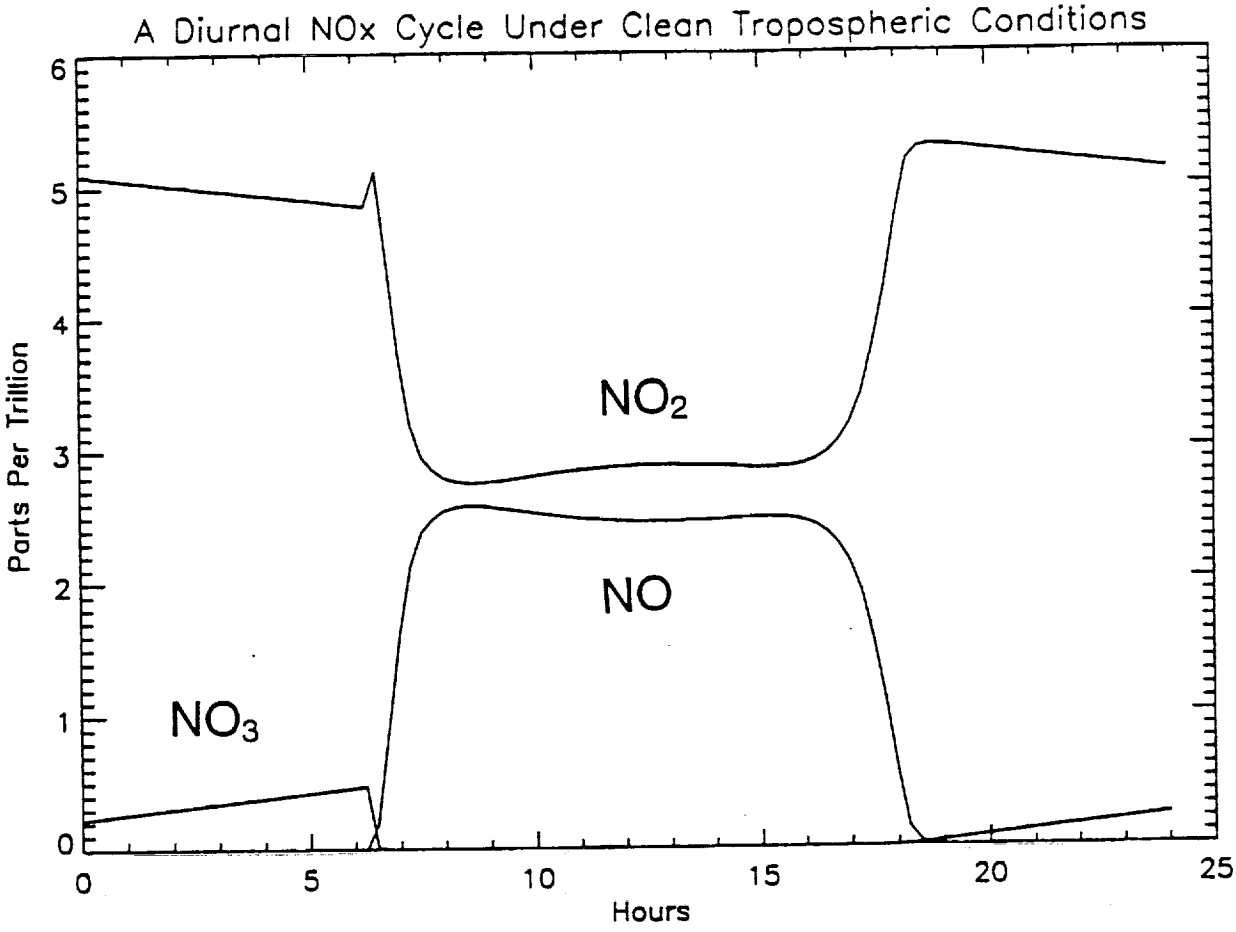
A Diurnal NOx Cycle Under Clean Tropospheric Conditions
Parts Per Trillion
Hours
NO2
NO
NO3
0
1
2
3
4
5
6
0
5
10
15
20
25

Figure 22a.

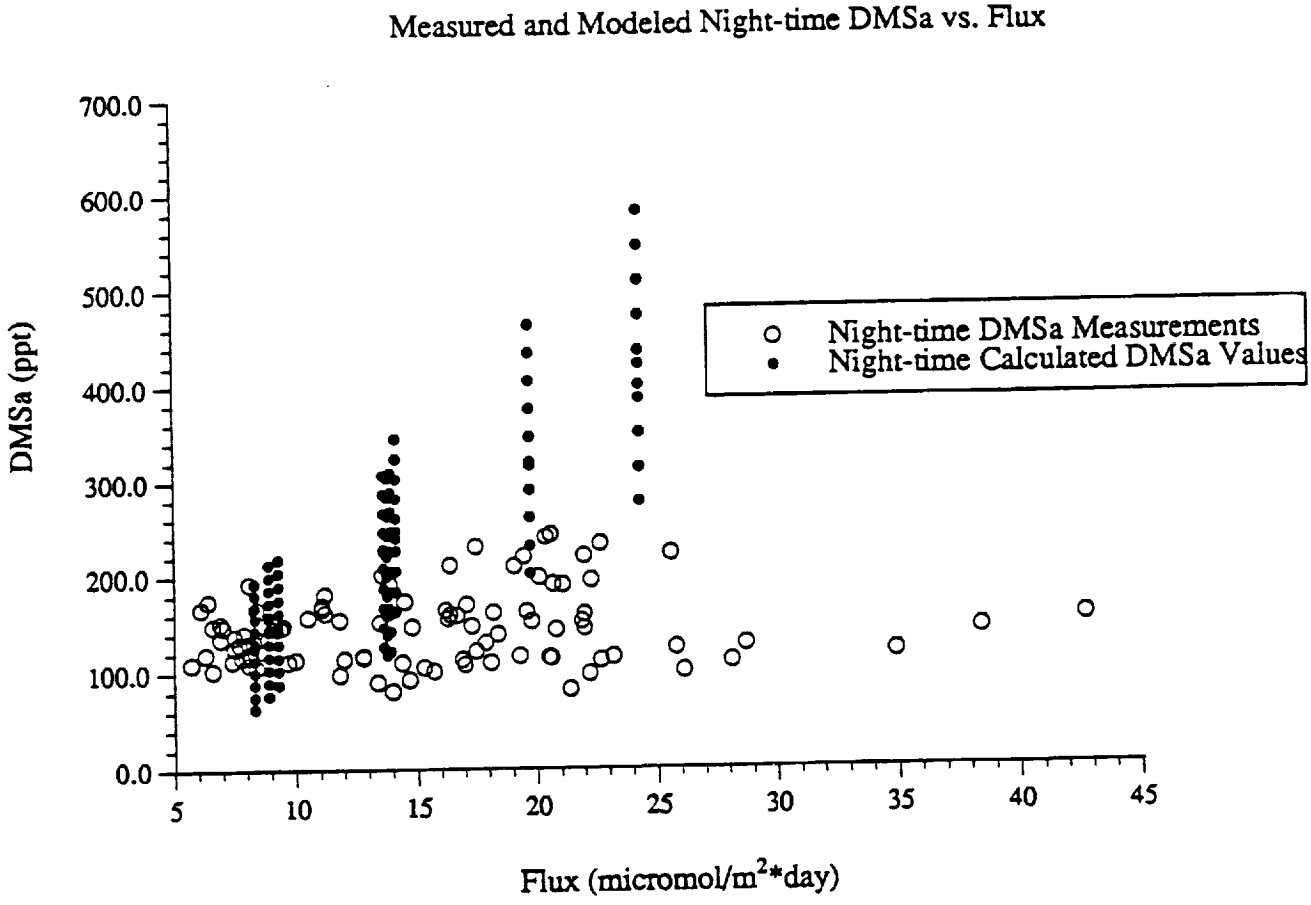
Measured and Modeled Night-time DMSa vs. Flux
DMSa (ppt)
700.0
600.0
500.0
400.0
300.0
200.0
100.0
0.0
5
10
15
20
25
30
35
40
45
Flux (micromol/m2*day)
Night-time DMSa Measurements
Night-time Calculated DMSa Values

Figure 22b.

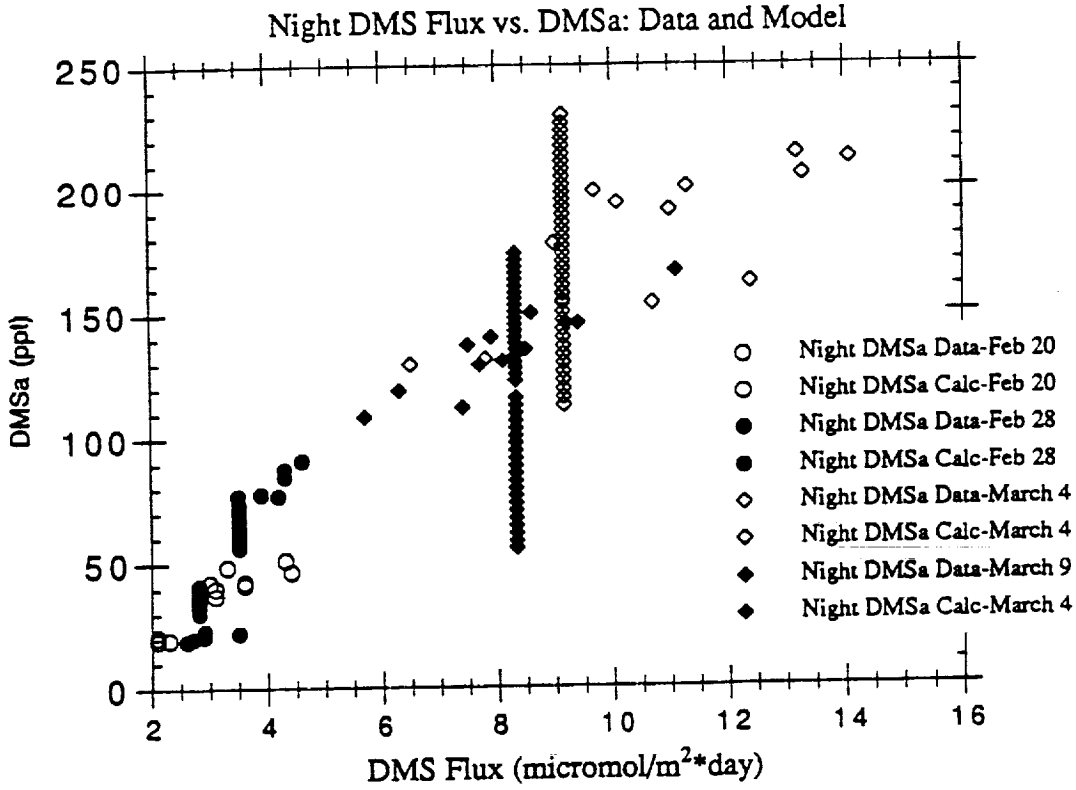
Night DMS Flux vs. DMSa: Data and Model
DMSa (ppl)
250
200
150
100
50
0
2
4
6
8
10
12
14
16
DMS Flux (micromol/m2*day)
Night DMSa Data-Feb 20
Night DMSa Calc-Feb 20
Night DMSa Data-Feb 28
Night DMSa Calc-Feb 28
Night DMSa Data-March 4
Night DMSa Calc-March 4
Night DMSa Data-March 9
Night DMSa Calc-March 4

Figure 23a.

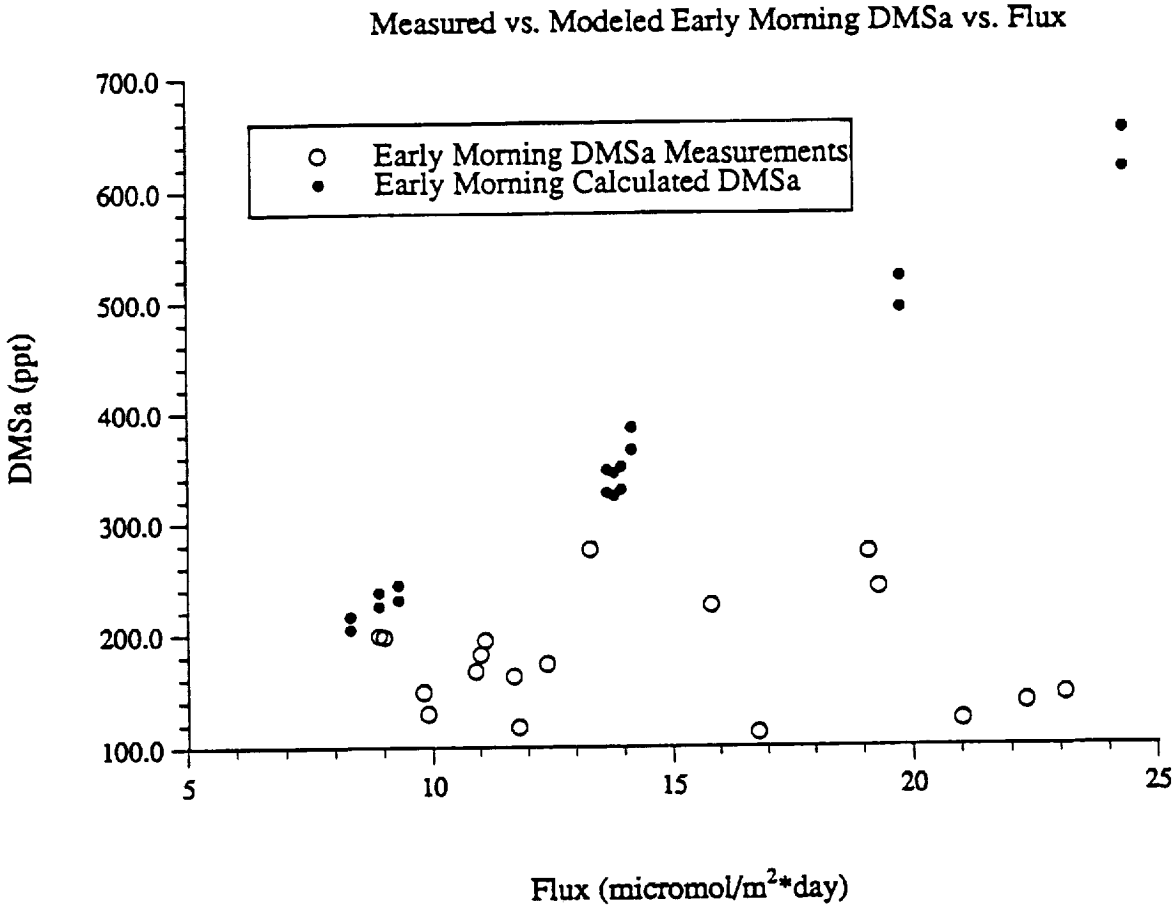
Measured vs. Modeled Early Morning DMSa vs. Flux
Early Morning DMSa Measurements
Early Morning Calculated DMSa
DMSa (ppt)
700.0
600.0
500.0
400.0
300.0
200.0
100.0
5
10
15
20
25
Flux (micromol/m2*day)

Figure 23b.

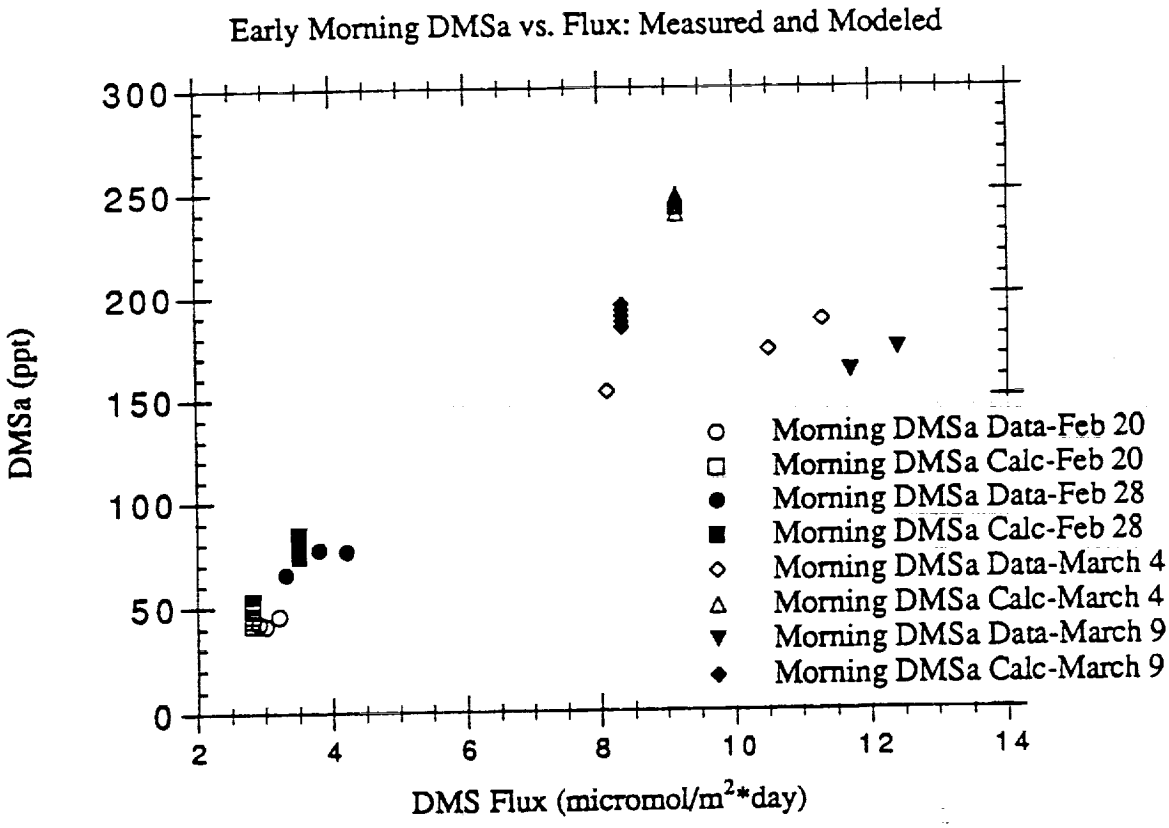
Early Morning DMSa vs. Flux: Measured and Modeled
DMSa (ppt)
300
250
200
150
100
50
0
2
4
6
8
10
12
14
DMS Flux (micromol/m2*day)
Morning DMSa Data-Feb 20
Morning DMSa Calc-Feb 20
Morning DMSa Data-Feb 28
Morning DMSa Calc-Feb 28
Morning DMSa Data-March 4
Morning DMSa Calc-March 4
Morning DMSa Data-March 9
Morning DMSa Calc-March 9

Figure 24a.

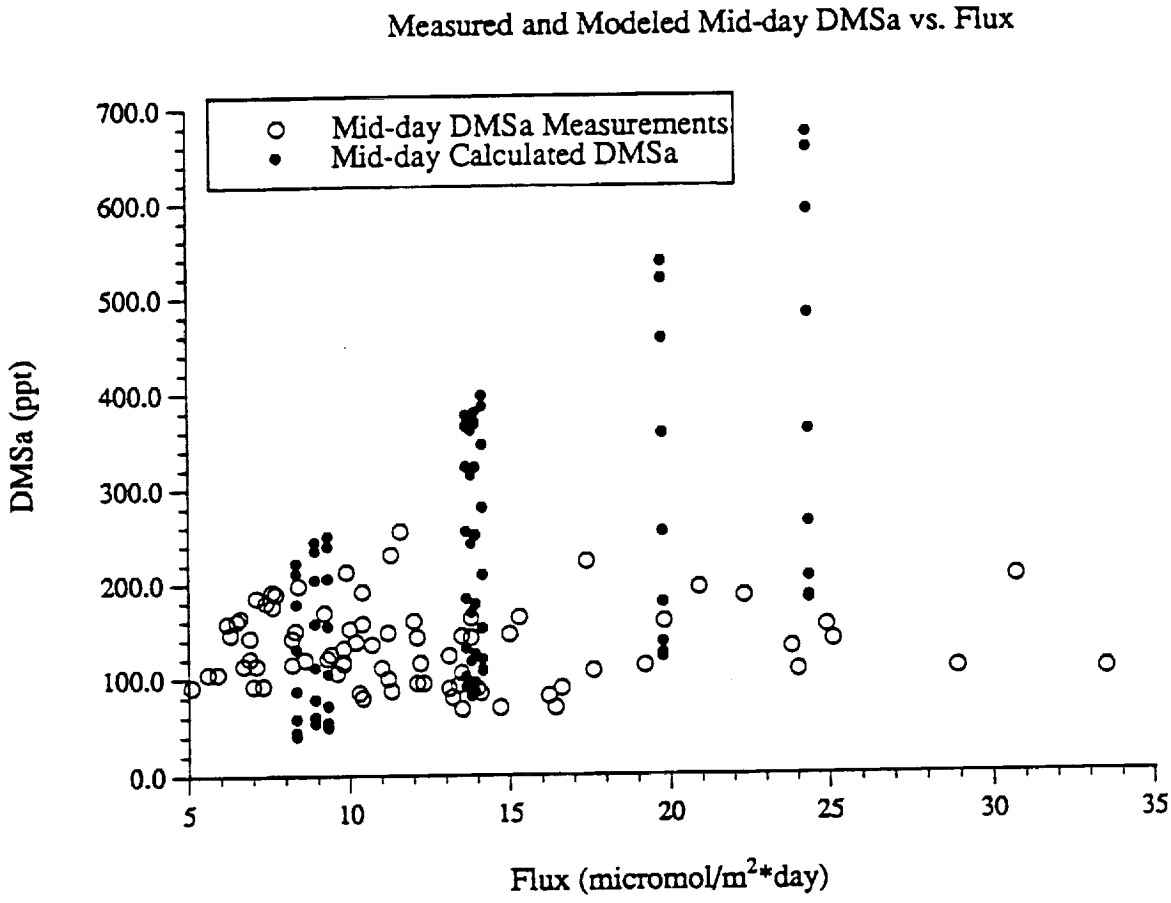
Measured and Modeled Mid-day DMSa vs. Flux
Mid-day DMSa Measurements
Mid-day Calculated DMSa
DMSa (ppt)
700.0
600.0
500.0
400.0
300.0
200.0
100.0
0.0
5
10
15
20
25
30
35
Flux (micromol/m2*day)

Figure 24b.

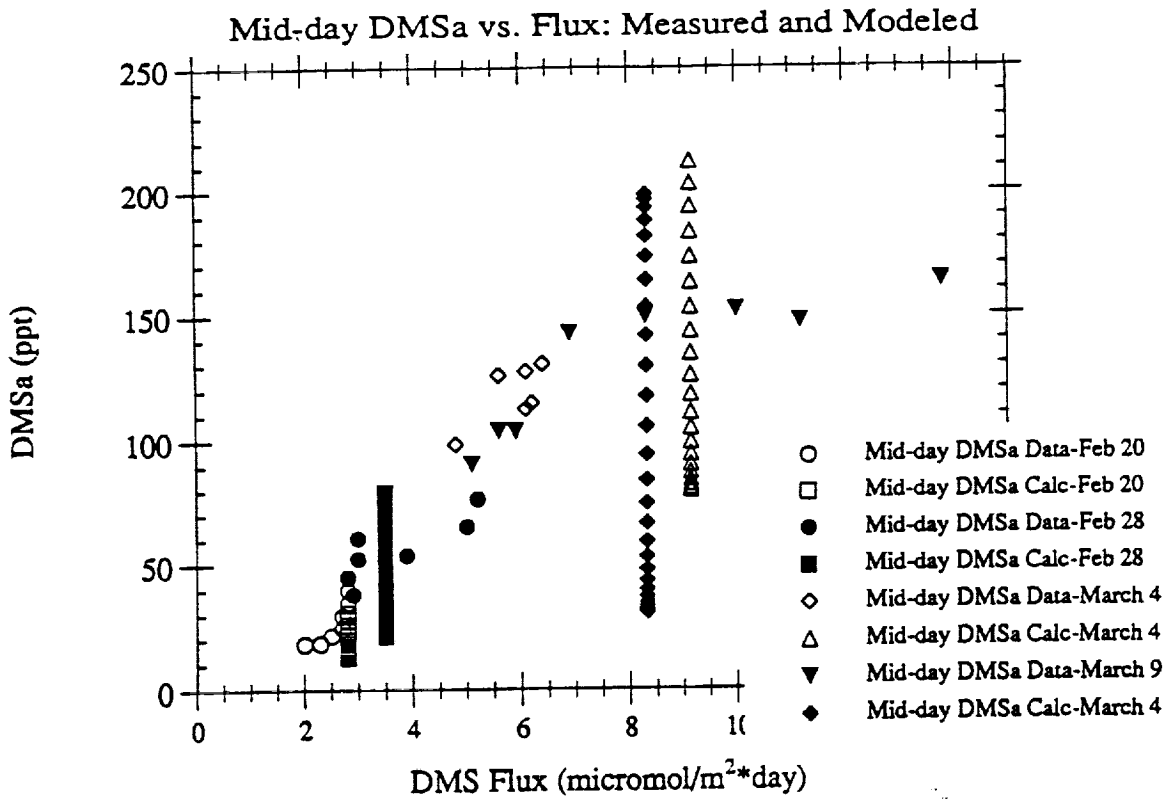
Mid-day DMSa vs. Flux: Measured and Modeled
DMSa (ppt)
250
200
150
100
50
0
0
2
4
6
8
DMS Flux (micromol/m2*day)
Mid-day DMSa Data-Feb 20
Mid-day DMSa Calc-Feb 20
Mid-day DMSa Data-Feb 28
Mid-day DMSa Calc-Feb 28
Mid-day DMSa Data-March 4
Mid-day DMSa Calc-March 4
Mid-day DMSa Data-March 9
Mid-day DMSa Calc-March 4

Figure 25a.

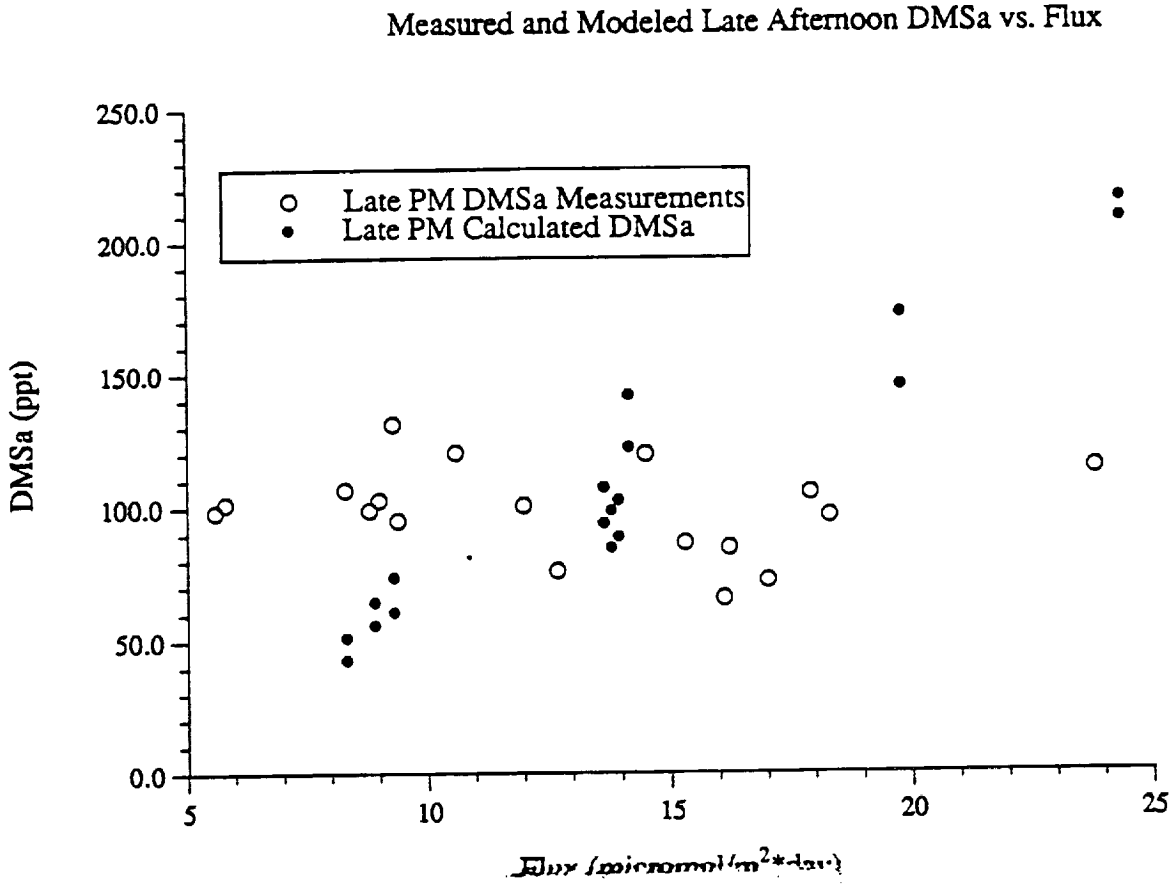
Measured and Modeled Late Afternoon DMSa vs. Flux
Late PM DMSa Measurements
Late PM Calculated DMSa
DMSa (ppt)
250.0
200.0
150.0
100.0
50.0
0.0
5
10
15
20
25

Figure 25b.

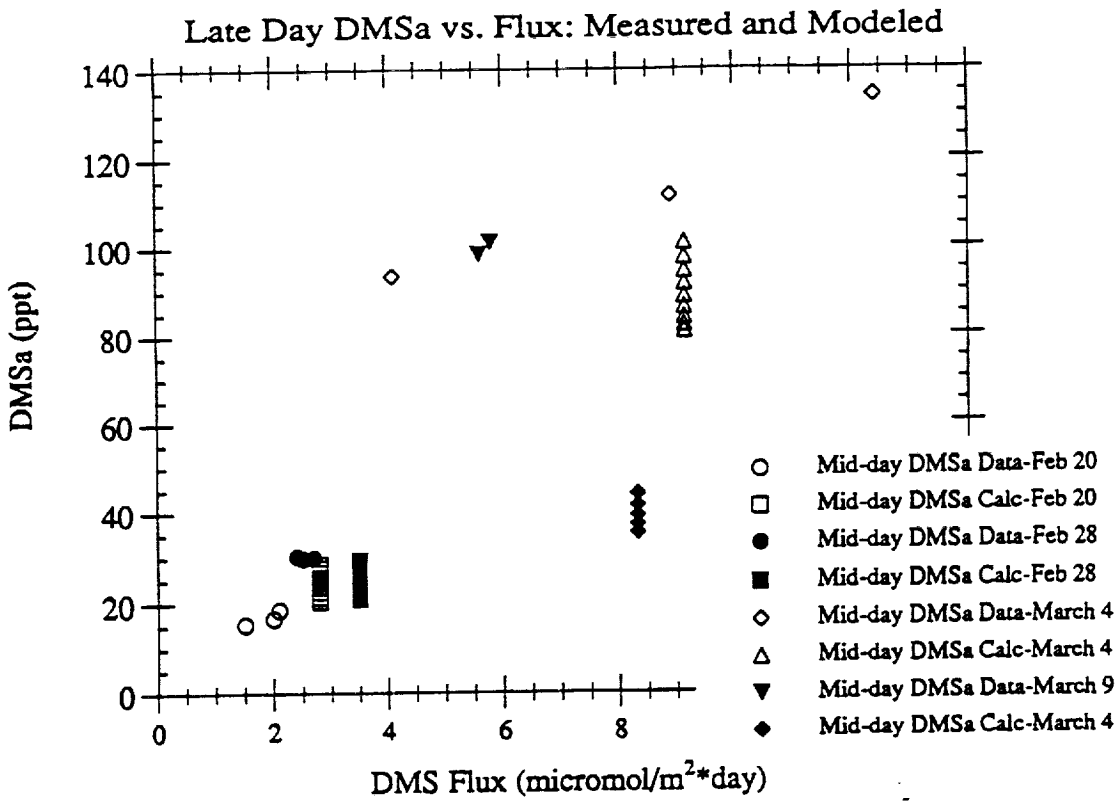
Late Day DMSa vs. Flux: Measured and Modeled
DMSa (ppt)
140
120
100
80
60
40
20
0
0
2
4
6
8
DMS Flux (micromol/m2*day)
Mid-day DMSa Data-Feb 20
Mid-day DMSa Calc-Feb 20
Mid-day DMSa Data-Feb 28
Mid-day DMSa Calc-Feb 28
Mid-day DMSa Data-March 4
Mid-day DMSa Calc-March 4
Mid-day DMSa Data-March 9
Mid-day DMSa Calc-March 4

Figure 26.

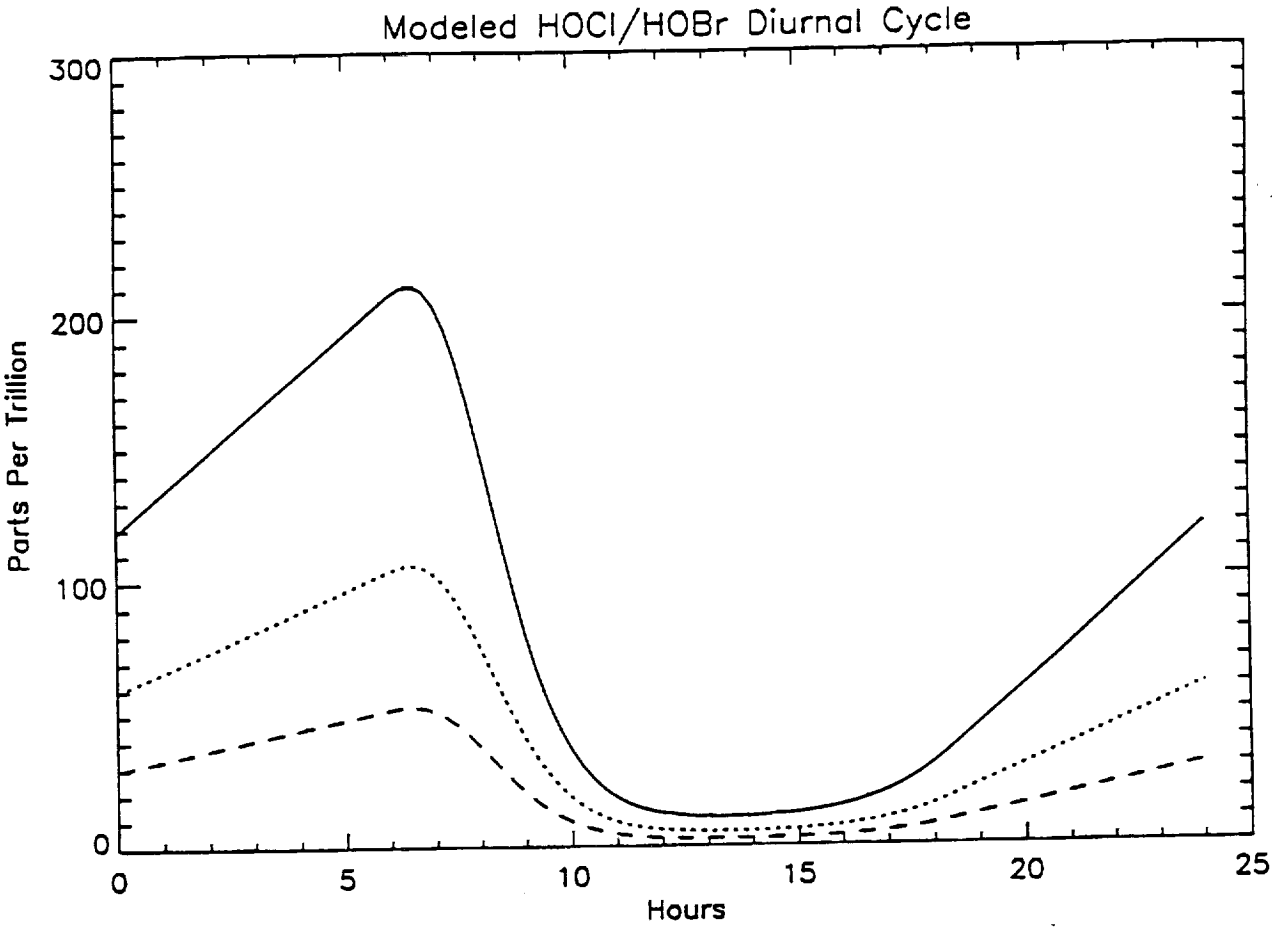
Modeled HOCl/HOBr Diurnal Cycle
Parts Per Trillion
300
200
100
0
0
5
10
15
20
25
Hours

Figure 27.

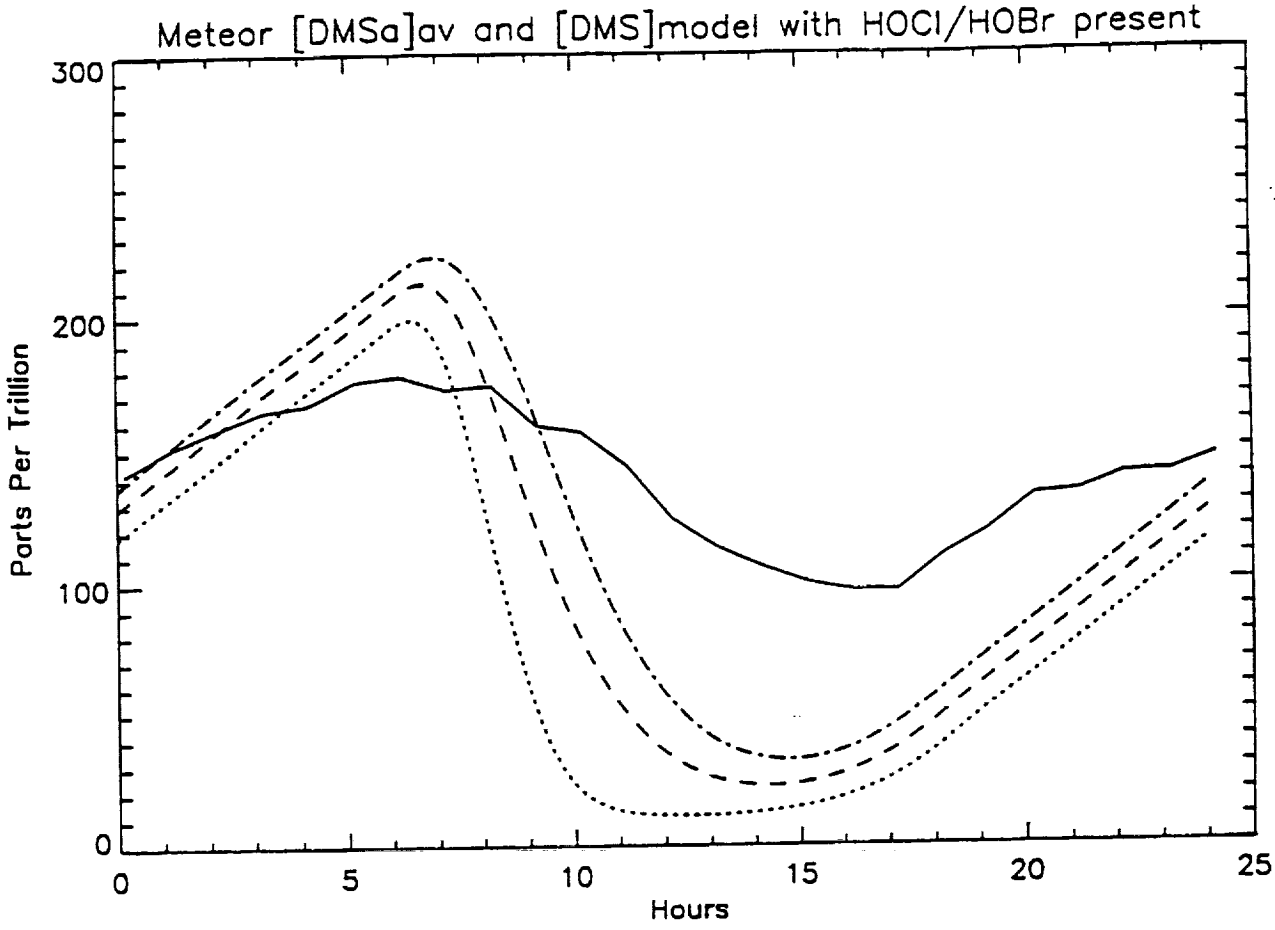
Meteor [DMSa]av and [DMS]model with HOCl/HOBr present
300
200
100
0
Parts Per Trillion
0
5
10
15
20
25
Hours